

# Electrophilic synthesis of [ $^{18}\text{F}$ ]UCB-J and evaluation of metabolic profile in rats

Department of Chemistry, Radiopharmaceutical Chemistry Research Group

Master's thesis

Author:

Joonas Pohja

2.12.2024

Turku

The originality of this thesis has been checked in accordance with the University of Turku quality assurance system using the Turnitin Originality Check service.

Master's thesis

**Subject:** Radiopharmaceutical Chemistry

**Author:** Joonas Pohja

**Title:** Electrophilic synthesis of [<sup>18</sup>F]UCB-J and evaluation of metabolic profile in rats

**Supervisors:** Thomas Keller, Anna Kirjavainen

**Number of pages:** 40 pages

**Date:** 2.12.2024

Positron emission tomography is a technique of non-invasive imaging of a body utilizing positron emitting radionuclides. Among the many radionuclides used in positron emission tomography, fluorine-18 has proven to be extremely suitable for it due to its beneficial properties of a relatively long half-life of 109.8 minutes and low maximum positron emission energy of 635 keV. Fluorine-18 can be used in the radiolabeling of compounds via either a nucleophilic or electrophilic approach. The use of electrophilic fluorine-18 labeling has the advantage of higher reactivity while suffering from lower molar activity when compared to the nucleophilic method. Several different electrophilic <sup>18</sup>F-fluorinating reagents have been developed to aid in the use of electrophilic fluorine-18, among them [<sup>18</sup>F]fluoro-benziodoxole.

[<sup>18</sup>F]Fluoro-benziodoxole is an electrophilic <sup>18</sup>F-fluorinating reagent capable of the umpolung of fluorine-18. This ability allows for the combining of the nucleophilic and electrophilic methods via an inversion of polarity, by first producing fluorine-18 as a nucleophile and then converting it to an electrophilic form. Due to this fluorine-18 can be produced in high starting molar activities afforded by the nucleophilic fluorine-18 and then utilizing the high reactivity of the electrophilic form. [<sup>18</sup>F]Fluoro-benziodoxole has not been widely applied in the field radiopharmaceutical chemistry, and one of the aims of this work is to test it in the synthesis of the radiotracer [<sup>18</sup>F]UCB-J.

[<sup>18</sup>F]UCB-J is a radiotracer for the imaging of synaptic vesicle glycoprotein 2A that has been previously used as mainly a carbon-11 labeled radiotracer but recently a fluorine-18 labeled version has also been developed. In addition to testing the use [<sup>18</sup>F]fluoro-benziodoxole for the synthesis of [<sup>18</sup>F]UCB-J, this work also includes a study of the radiometabolism of [<sup>18</sup>F]UCB-J using rats as test animals.

When comparing the results of the [<sup>18</sup>F]fluoro-benziodoxole synthesis of [<sup>18</sup>F]UCB-J to the reference HPLC chromatogram, no produced [<sup>18</sup>F]UCB-J could be detected. This shows that the [<sup>18</sup>F]fluoro-benziodoxole synthesis of [<sup>18</sup>F]UCB-J does not work. The analyzed results of the radiometabolism study of [<sup>18</sup>F]UCB-J were analyzed by reverse and normal phase radioTLC and radioHPLC. The results of the radiometabolism study show large degrees of radiometabolism in the liver and plasma of the test animals while showing the least radiometabolism in the brain and liver of the test animals. In addition to this the reverse phase radioTLC method afforded better separation of radiometabolites than the normal phase radioTLC method.

Though the synthesis of [<sup>18</sup>F]UCB-J via the [<sup>18</sup>F]fluoro-benziodoxole method was not successful, [<sup>18</sup>F]fluoro-benziodoxole should not be ruled out as an electrophilic <sup>18</sup>F-fluorinating reagent. Further testing is required to chart the full potential uses of [<sup>18</sup>F]fluoro-benziodoxole in the field of fluorine-18 radiolabeling chemistry.

**Key words:** positron emission tomography, fluorine-18, [<sup>18</sup>F]fluoro-benziodoxole, [<sup>18</sup>F]UCB-J, radiometabolism.

# Table of contents

<b>1</b>	<b>Introduction</b>	<b>1</b>
<b>1.1</b>	<b>Fluorine-18</b>	<b>1</b>
1.1.1	Fluorine-18 production	1
<b>1.2</b>	<b>Electrophilic fluorine-18 labeling</b>	<b>2</b>
1.2.1	[ <sup>18</sup> F]F <sub>2</sub> gas	2
1.2.2	[ <sup>18</sup> F]CF <sub>3</sub> OF	3
1.2.3	[ <sup>18</sup> F]FCIO <sub>3</sub>	3
1.2.4	[ <sup>18</sup> F]CH <sub>3</sub> COOF	4
1.2.5	[ <sup>18</sup> F]XeF <sub>2</sub>	4
1.2.6	1-[ <sup>18</sup> F]Fluoro-2-pyridone	5
1.2.7	N-[ <sup>18</sup> F]Fluoro-N-alkylsulfonamides	6
1.2.8	N-[ <sup>18</sup> F]fluorobenzenesulfonimide ([ <sup>18</sup> F]NFSI)	6
1.2.9	N-[ <sup>18</sup> F]Fluoropyridinium triflate	7
1.2.10	[ <sup>18</sup> F]Selectfluor bis(triflate)	7
1.2.11	Transition metal electrophilic <sup>18</sup> F-fluorination reagents	8
1.2.12	[ <sup>18</sup> F]Fluoro-benziodoxole	10
<b>1.3</b>	<b>UCB-J</b>	<b>11</b>
<b>2</b>	<b>Experiment</b>	<b>12</b>
<b>2.1</b>	<b>Aims of the work</b>	<b>12</b>
<b>2.2</b>	<b>Synthesis of [<sup>18</sup>F]fluoro-benziodoxole precursors</b>	<b>12</b>
<b>2.3</b>	<b>Synthesis of [<sup>18</sup>F]UCB-J</b>	<b>13</b>
2.3.1	[ <sup>18</sup> F]Tetrabutylammonium fluoride production	14
2.3.2	[ <sup>18</sup> F]UCB-J production	14
<b>2.4</b>	<b>[<sup>18</sup>F]UCB-J radiometabolism in rats</b>	<b>15</b>
2.4.1	[ <sup>18</sup> F]UCB-J synthesis	15
2.4.2	[ <sup>18</sup> F]UCB-J radiometabolism studies	16
<b>3</b>	<b>Results</b>	<b>18</b>
3.1.1	Synthesis of [ <sup>18</sup> F]Fluoro-benziodoxole precursors	18
3.1.2	[ <sup>18</sup> F]UCB-J synthesis via [ <sup>18</sup> F]fluoro-benziodoxole	19
3.1.3	Selectfluor synthesis of [ <sup>18</sup> F]UCB-J for metabolism studies	23
3.1.4	Biodistribution of injected activity	23
3.1.5	Radiometabolism study	24
<b>4</b>	<b>Conclusions</b>	<b>30</b>
<b>5</b>	<b>References</b>	<b>32</b>

**6 Attachments 36**

**6.1 List of attachments: 36**

## **Abbreviations**

PET      Positron Emission Tomography

FDG      Fluorodeoxyglucose

DOPA    Dihydroxyphenylalanine

RA       Radioactivity

UV       Ultraviolet

RP       Reverse phase

NP       Normal phase

# 1 Introduction

Positron emission tomography (PET) is an imaging technique utilizing radioactivity that can be used for the study and diagnosis of the body in the medical field. The basic principle of PET imaging is the utilization of the annihilation reaction between an emitted positron and an electron. Positron emitting radionuclides are bound to a radiotracer that targets a specific site in the body. The annihilation creates two gamma photons of 511 keV in opposite directions. An image of the distribution of the positron emitters in the body can be created by detecting the photons. This way various sites in the body can be studied in a non-invasive way. A variety of positron emitting radionuclides are utilized in PET imaging, some of the most prominent being fluorine-18, carbon-11 and gallium-68. Among them fluorine-18 is a radionuclide of interest for its relatively long half-life of 109.8 minutes and the relatively low maximum positron of energy of 635 keV. These qualities give fluorine-18 an advantage over other positron emitting radionuclides by affording more synthesis and transport time and yielding better spatial resolution when used in PET imaging.

## 1.1 Fluorine-18

Fluorine-18 can be used in radiolabeling with two different main methods, either nucleophilically or electrophilically. Both  $^{18}\text{F}$ -fluorination methods have their advantages and downsides. Nucleophilic fluorine-18 can be generally produced in higher starting molar activities than electrophilic fluorine-18, but it is less reactive than electrophilic fluorine-18. The reactivity of electrophilic fluorine-18 can also be a downside leading to lower regioselectivity. Electrophilic fluorine-18 is most commonly produced via two different nuclear reactions using a cyclotron.

### 1.1.1 Fluorine-18 production

The  $^{20}\text{Ne}(\text{d},\alpha)^{18}\text{F}$  reaction produces electrophilic fluorine-18 from neon gas while the  $^{18}\text{O}(\text{p},\text{n})^{18}\text{F}$  reaction uses a gaseous  $[^{18}\text{O}]\text{O}_2$  target to produce electrophilic fluorine-18 or a liquid  $[^{18}\text{O}]\text{H}_2\text{O}$  target to produce nucleophilic fluorine-18. In both reactions the target,  $^{20}\text{Ne}$  or  $^{18}\text{O}$  is bombarded by cyclotron accelerated particles. Another method utilizing the  $^6\text{Li}(\text{n},\alpha)^3\text{H}$  and subsequent  $^{16}\text{O}(\text{t},\text{n})^{18}\text{F}$  nuclear reactions to produce nucleophilic fluorine-18 also exists. In this method the target lithium is activated by thermal neutron bombardment causing it to emit tritiums that are used in the  $^{16}\text{O}(\text{t},\text{n})^{18}\text{F}$  nuclear reaction.<sup>1</sup> When using the  $^{20}\text{Ne}(\text{d},\alpha)^{18}\text{F}$  or  $^{18}\text{O}(\text{p},\text{n})^{18}\text{F}$  reactions for electrophilic fluorine-18 production stable carrier fluorine isotope fluorine-19 needs to be added to form the desired  $[^{18}\text{F}]\text{F}_2$  gas. This added carrier reduces the molar activity that can be obtained when compared to producing nucleophilic fluorine-18. This addition of fluorine-19 is also the reason that  $[^{18}\text{F}]\text{F}_2$  gas has a

maximum radiochemical yield of only 50% as only half of the produced fluorine is fluorine-18. The main focus of this work is various different methods employed in electrophilic fluorine-18 labeling, starting with the simplest method of direct  $^{18}\text{F}$ -fluorination via  $[^{18}\text{F}]\text{F}_2$  gas.

## 1.2 Electrophilic fluorine-18 labeling

### 1.2.1 $[^{18}\text{F}]\text{F}_2$ gas

To address the problem of low starting molar activities when producing electrophilic fluorine-18 a post-target method utilizing a high voltage electrical discharge has been developed by Bergmann and Solin<sup>2</sup>. In this method fluorine-18 is produced in nucleophilic fluoride-18 form via the  $^{18}\text{O}(\text{p},\text{n})^{18}\text{F}$  nuclear reaction using oxygen-18 enriched water as the irradiation target. The produced  $[^{18}\text{F}]\text{F}^-$  is then dried azeotropically in a reaction vessel containing potassium carbonate, kryptofix 2.2.2 and acetonitrile. After drying methyl iodide is added to form  $[^{18}\text{F}]\text{methyl fluoride}$  ( $[^{18}\text{F}]\text{CH}_3\text{F}$ ) as a gas which is purified and then trapped in a stainless steel loop via cooling. After collection the  $[^{18}\text{F}]\text{CH}_3\text{F}$  is then transferred to a discharge chamber using neon sweep gas that contains a known amount of carrier fluorine-19. In the discharge chamber a high voltage discharge of 20-30 kV is used to break the bonds of the carrier fluorine-19  $\text{F}_2$  gas and the  $[^{18}\text{F}]\text{CH}_3\text{F}$  leading to reformation of the molecules. This reformation affords  $[^{18}\text{F}]\text{F}_2$  gas in molar activities of up to 55 GBq  $\mu\text{mol}^{-1}$ , higher than what can be achieved via cyclotron produced  $[^{18}\text{F}]\text{F}_2$  gas.<sup>2</sup> This method is presented in figure 1. Using similar methodology but substituting the high voltage discharge for UV photons generated by an excimer laser has also been successful<sup>3</sup>.

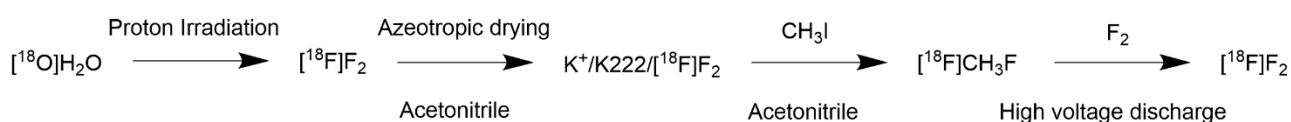


Figure 1: Post-target synthesis of  $[^{18}\text{F}]\text{F}_2$  using high voltage discharge

Though  $[^{18}\text{F}]\text{F}_2$  gas is used by itself in labeling of certain radiopharmaceuticals such as 6- $[^{18}\text{F}]\text{fluoro-L-DOPA}$ <sup>4</sup> and  $[^{18}\text{F}]\text{FDG}$ <sup>5</sup>, it is an extremely reactive molecule with poor regioselectivity. In order to improve the regioselectivity of the electrophilic  $^{18}\text{F}$ -fluorination many different kinds of  $^{18}\text{F}$ -fluorinating reagents have been developed to curtail the reactivity of  $[^{18}\text{F}]\text{F}_2$  gas and open a wider variety of radiopharmaceuticals for production via electrophilic fluorine-18.

### 1.2.2 [<sup>18</sup>F]CF<sub>3</sub>OF

One of the first electrophilic fluorinating reagents developed was [<sup>18</sup>F]trifluoromethyl hypofluorite ([<sup>18</sup>F]CF<sub>3</sub>OF) (fig.2). [<sup>18</sup>F]CF<sub>3</sub>OF can be produced from [<sup>18</sup>F]F<sub>2</sub> gas and CF<sub>2</sub>O using CsF or KF as a catalyst. In this method a NiF<sub>2</sub> coated target is filled with 0.5 g of the catalytic material, either CsF or KF, and then filled with 2000 mmHg of neon gas after which it was irradiated by 10.4 MeV deuterons to produce [<sup>18</sup>F]F<sub>2</sub> gas. After the bombardment and evacuation of excess Ne, F<sub>2</sub> gas and CF<sub>2</sub>O are added to form [<sup>18</sup>F]CF<sub>3</sub>OF. Using this method 97% of the CF<sub>2</sub>O starting material was found to be converted to CF<sub>3</sub>OF when using a CsF catalyst with a 1:0.9 ratio of F<sub>2</sub> and CF<sub>2</sub>O. Of the received activity 98% was determined to be [<sup>18</sup>F]CF<sub>3</sub>OF and 2% of the activity being the side product [<sup>18</sup>F]CF<sub>3</sub>OOCF<sub>3</sub> and less than 0.05% to be from the side product [<sup>18</sup>F]CF<sub>4</sub>.<sup>6</sup> [<sup>18</sup>F]CF<sub>3</sub>OF is not as reactive as [<sup>18</sup>F]F<sub>2</sub> gas and tolerates water making it a more suitable fluorinating reagent for use in synthesis of radiolabeled molecules<sup>7</sup>. One of the down sides of this method is that only a third of the [<sup>18</sup>F]CF<sub>3</sub>OF activity is in the -OF part of [<sup>18</sup>F]CF<sub>3</sub>OF. This hypofluorite function is the one that contains the electrophilic fluorine and this fact has a lowering effect on radiochemical yields when using [<sup>18</sup>F]CF<sub>3</sub>OF to produce radiolabeled molecules.<sup>6</sup>

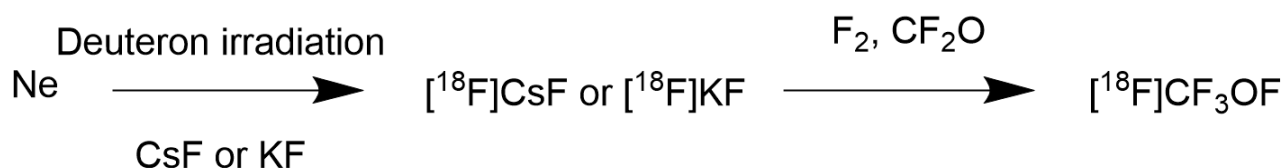


Figure 2: [<sup>18</sup>F]CF<sub>3</sub>OF synthesis

### 1.2.3 [<sup>18</sup>F]FCIO<sub>3</sub>

Another electrophilic <sup>18</sup>F-fluorinating reagent is [<sup>18</sup>F]perchloryl fluoride ([<sup>18</sup>F]FCIO<sub>3</sub>) (fig. 3) that can be used particularly in the <sup>18</sup>F-fluorination of aryl-lithium structures. [<sup>18</sup>F]FCIO<sub>3</sub> was first synthesized<sup>8</sup> by producing [<sup>18</sup>F]F<sub>2</sub> gas via the <sup>20</sup>Ne(d,α)<sup>18</sup>F nuclear reaction and then reacting the produced [<sup>18</sup>F]F<sub>2</sub> gas with KClO<sub>3</sub> in column at 90°C by rapid gas flow of 200 ml/min. Produced [<sup>18</sup>F]FCIO<sub>3</sub> gas was purified by flowing it through two solid phase scrubbers, one containing NaOH and the other Na<sub>2</sub>S<sub>2</sub>O<sub>3</sub>. Using this method [<sup>18</sup>F]FCIO<sub>3</sub> could be produced in average yields of 23% regardless of the reaction parameters such as concentration of carrier F<sub>2</sub>, temperature or purge gas flow rate.<sup>8</sup> The major downside of [<sup>18</sup>F]FCIO<sub>3</sub> is that it is a strong oxidant capable of exploding<sup>9</sup>, adding an extra safety consideration when utilized for <sup>18</sup>F-fluorination.

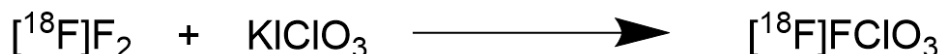


Figure 3: Synthesis  $[^{18}\text{F}]\text{FCIO}_3$

$[^{18}\text{F}]\text{Perchloryl fluoride}$  has been used in the synthesis of 2- $[^{18}\text{F}]\text{fluoro-diethyl malonate}$  and  $[^{18}\text{F}]\text{fluorobenzene}$ , but these resulted in low radiochemical yields due to a different no carrier added method that was used for  $[^{18}\text{F}]\text{perchloryl fluoride}$  production.<sup>10</sup>

#### 1.2.4 $[^{18}\text{F}]\text{CH}_3\text{COOF}$

$[^{18}\text{F}]\text{Acetyl hypofluorite}$  ( $[^{18}\text{F}]\text{CH}_3\text{COOF}$ ) (fig. 4) is an electrophilic  $^{18}\text{F}$ -fluorinating reagent that was first synthesized<sup>11</sup> by producing  $[^{18}\text{F}]\text{F}_2$  gas through the  $^{20}\text{Ne}(d,\alpha)^{18}\text{F}$  reaction and bubbling the product through a mixture containing 950  $\mu\text{mol}$  of ammonium acetate in 15 ml of anhydrous acetic acid. This method was used in conjunction with producing 6- $[^{18}\text{F}]\text{fluoro-L-DOPA}$  radiotracer which necessitated the use of acetic acid as a solvent<sup>11</sup>, but  $\text{CFCl}_3$  can also be used in the synthesis of  $[^{18}\text{F}]\text{CH}_3\text{COOF}$ <sup>12</sup>. Compared with previously discussed electrophilic  $^{18}\text{F}$ -fluorinating reagents  $[^{18}\text{F}]\text{CH}_3\text{COOF}$  is dissolved in solution and not in gaseous state at room temperature allowing for easier handling of produced activity.<sup>11</sup>  $[^{18}\text{F}]\text{CH}_3\text{COOF}$  is capable of  $^{18}\text{F}$ -labeling aryl-tin compounds by cleavage of the aryl-tin bond<sup>13</sup>.

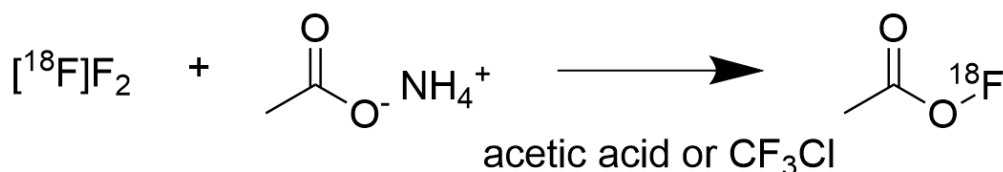


Figure 4: Synthesis of  $[^{18}\text{F}]\text{CH}_3\text{COOF}$

$[^{18}\text{F}]\text{CH}_3\text{COOF}$  has been used for the synthesis of many radiolabeled compounds, such as the previously mentioned 6- $[^{18}\text{F}]\text{fluoro-L-DOPA}$ <sup>14,15,16,17,18</sup> as well as  $[^{18}\text{F}]\text{FDG}$ <sup>19,20</sup>, 4-borono-2- $[^{18}\text{F}]\text{fluoro-L-phenylalanine-fructose}$ <sup>21</sup> and  $[^{18}\text{F}]\text{2-oxoquazepam}$ <sup>22</sup>. In addition to these,  $[^{18}\text{F}]\text{CH}_3\text{COOF}$  has been used to synthesize a variety of  $^{18}\text{F}$ -labelled N,N-dimethylamphetamine analogues<sup>23</sup> and 5-fluoro-5,6-dihydrouracil nucleosides<sup>24</sup> as well as 2-deoxy-2-( $[^{18}\text{F}]\text{fluoro}$ )-D-galactopyranose<sup>25</sup> and both 6- $[^{18}\text{F}]\text{-}$  and 4- $[^{18}\text{F}]\text{fluoro-L-m-tyrosines}$ <sup>26</sup>.

#### 1.2.5 $[^{18}\text{F}]\text{XeF}_2$

$[^{18}\text{F}]\text{Xenon difluoride}$  ( $[^{18}\text{F}]\text{XeF}_2$ ) is a milder electrophilic  $^{18}\text{F}$ -fluorinating reagent than  $[^{18}\text{F}]\text{F}_2$  gas<sup>27</sup>.  $[^{18}\text{F}]\text{XeF}_2$  was first synthesized<sup>28</sup> by utilizing an isotopic exchange of fluorine between  $\text{XeF}_2$  and  $[^{18}\text{F}]\text{HF}$ ,  $[^{18}\text{F}]\text{AsF}_5$  or  $[^{18}\text{F}]\text{SiF}_4$ . In this method fluorine-18 is first produced as  $[^{18}\text{F}]\text{F}^-$  via the

${}^6\text{Li}(n,\alpha){}^3\text{H}$  and subsequent  ${}^{16}\text{O}(t,n){}^{18}\text{F}$  nuclear reactions<sup>1</sup> where  $[{}^6\text{Li}]\text{Li}_2\text{CO}_3$  is bombarded with thermal neutrons and then dissolved in 4 M sulfuric acid. This solution was then heated and water that contained  $[{}^{18}\text{F}]\text{HF}$  and trace amounts of sulfuric acid was distilled from the solution. The distilled water was then neutralized by addition of aqueous  $\text{Bu}_4\text{NOH}$  and evaporated to dryness in a vacuum at  $50^\circ\text{C}$  creating a residue of  $[{}^{18}\text{F}]\text{Bu}_4\text{NF}$  and  $(\text{Bu}_4\text{N})_2\text{SO}_4$ . This residue was then dissolved in dry acetonitrile and evaporated to dryness at  $40^\circ\text{C}$  in a vacuum. Afterwards spectroscopic grade  $\text{SO}_2\text{ClF}$  was condensed on the resulting residue at a temperature of  $-196^\circ\text{C}$ . Afterwards anhydrous HF was condensed on to the residue as well and the mixture was heated to  $40^\circ\text{C}$  for 20 minutes.  $\text{SO}_2\text{ClF}$  and  $[{}^{18}\text{F}]\text{HF}$  were then vacuum distilled from this solution to a vessel that contained  $\text{XeF}_2$  and heated for 20 minutes at  $40^\circ\text{C}$  to allow for the exchange of fluoride between  $\text{XeF}_2$  and  $[{}^{18}\text{F}]\text{HF}$ . After heating  $\text{SO}_2\text{ClF}$  and HF were removed by dynamic vacuum at  $-48^\circ\text{C}$  affording  $[{}^{18}\text{F}]\text{XeF}_2$ . This method was tested to also work using  $\text{AsF}_5$  or  $\text{SiF}_4$  in place of HF.<sup>28</sup> Figure 5 shows this method for production of  $[{}^{18}\text{F}]\text{XeF}_2$ .

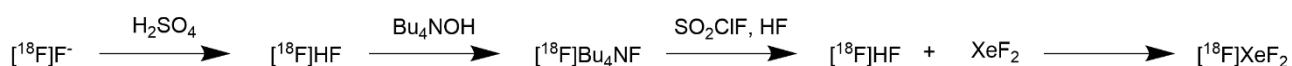


Figure 5: Synthesis of  $[{}^{18}\text{F}]\text{XeF}_2$  utilizing isotopic exchange

Another less complicated method to synthesize  $[{}^{18}\text{F}]\text{XeF}_2$  was developed<sup>29</sup> by producing  $[{}^{18}\text{F}]\text{F}_2$  gas via the  ${}^{20}\text{Ne}(d,\alpha){}^{18}\text{F}$  nuclear reaction and then transferring the  $[{}^{18}\text{F}]\text{F}_2$  gas to a high pressure nickel vessel that had been charged with xenon gas. The nickel vessel was then heated for 30 minutes at  $390^\circ\text{C}$  after which it was cooled to  $-40^\circ\text{C}$  affording  $[{}^{18}\text{F}]\text{XeF}_2$  and unreacted neon, xenon and  $[{}^{18}\text{F}]\text{F}_2$  gasses were released.  $[{}^{18}\text{F}]\text{XeF}_2$  produced via this method was used for the  ${}^{18}\text{F}$ -fluorination of  $[{}^{18}\text{F}]\text{2-fluoro-2-deoxy-D-glucose}$ .<sup>29</sup>  $[{}^{18}\text{F}]\text{XeF}_2$  is a solid at room temperature and this allows for an easier handling when compared to gaseous electrophilic  ${}^{18}\text{F}$ -fluorinating reagents. Figure 6 shows this method for production of  $[{}^{18}\text{F}]\text{XeF}_2$ .  $[{}^{18}\text{F}]\text{XeF}_2$  has been previously used in the successful synthesis of  $[{}^{18}\text{F}]\text{FDG}$ .<sup>29</sup>



Figure 6: Synthesis of  $[{}^{18}\text{F}]\text{XeF}_2$  utilizing  $[{}^{18}\text{F}]\text{F}_2$  gas as starting material

### 1.2.6 1- $[{}^{18}\text{F}]\text{Fluoro-2-pyridone}$

1- $[{}^{18}\text{F}]\text{Fluoro-2-pyridone}$  (fig. 7) is an electrophilic  ${}^{18}\text{F}$ -fluorinating reagent capable of fluorinating organo-lithium compounds. 1- $[{}^{18}\text{F}]\text{Fluoro-2-pyridone}$  was first prepared by bubbling  $[{}^{18}\text{F}]\text{F}_2$  gas prepared via the  ${}^{20}\text{Ne}(d,\alpha){}^{18}\text{F}$  reaction through a solution of 2-(trimethylsiloxy)-pyridine in  $\text{CFCl}_3$  at a temperature of  $-78^\circ\text{C}$ . After reaction the produced crude 1- $[{}^{18}\text{F}]\text{Fluoro-2-pyridone}$  could be purified

using direct sublimation without a significant loss of its reactivity or purity and achieving purities greater than 92%. Yields of up to 48% could be achieved using this method with a synthesis time of 35 minutes.<sup>30</sup>

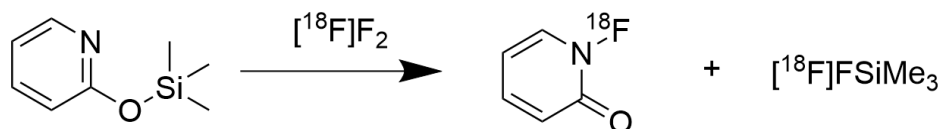


Figure 7: Synthesis of 1-<sup>18</sup>F-fluoro-2-pyridone

### 1.2.7 N-<sup>18</sup>F-Fluoro-N-alkylsulfonamides

N-<sup>18</sup>F-Fluoro-N-alkylsulfonamides are a group of electrophilic <sup>18</sup>F-fluorinating reagents that have the general chemical formula of  $\text{RSO}_2^{18}\text{FNR}'$ , where R and R' are various alkyl structures. N-<sup>18</sup>F-Fluoro-N-alkylsulfonamides were first synthesized<sup>31</sup> by producing  $[^{18}\text{F}]\text{F}_2$  gas via the  $^{20}\text{Ne}(\text{d},\alpha)^{18}\text{F}$  nuclear reaction and bubbled through a solution of sulfonamide ( $\text{RSO}_2\text{HNR}'$ ) in  $\text{CFCl}_3$  at a temperature of  $-78^\circ\text{C}$ . After this, the solvent was evaporated by passing nitrogen gas through the solution at room temperature and the remaining residue was dissolved in anhydrous diethyl ether and analyzed using radioHPLC and radioTLC. This method is presented in figure 8. Using this method radiochemical yields of up to 45% were achieved. N-<sup>18</sup>F-Fluoro-N-alkylsulfonamides produced this way were found to be capable of <sup>18</sup>F-fluorination of various Grignard and organolithium reagents.<sup>31</sup>

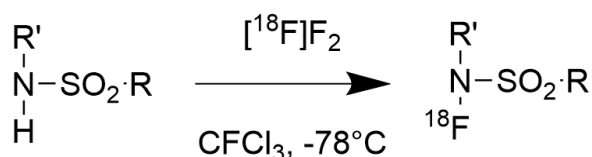


Figure 8: Synthesis of N-<sup>18</sup>F-fluoro-N-alkylsulfonamides

### 1.2.8 N-<sup>18</sup>F-fluorobenzenesulfonimide (<sup>18</sup>F]NFSI)

N-<sup>18</sup>F-fluorobenzenesulfonimide (<sup>18</sup>F]NFSI) (fig. 9) is another <sup>18</sup>F]N-F type electrophilic <sup>18</sup>F-fluorinating reagent like 1-<sup>18</sup>F-Fluoro-2-pyridone. It was first synthesized<sup>32</sup> by producing  $[^{18}\text{F}]\text{F}_2$  gas through the  $^{18}\text{O}(\text{p},\text{n})^{18}\text{F}$  nuclear reaction with 0.2% added carrier  $\text{F}_2$ .  $[^{18}\text{F}]\text{F}_2$  gas produced this way was then passed through a 0.01 M  $\text{NaN}(\text{SO}_2\text{Ph})_2$  solution in acetonitrile and water [9:1] for 10 minutes affording a crude product. An impurity of  $[^{18}\text{F}]\text{NaF}$  was detected but it does not interfere with the electrophilic <sup>18</sup>F-fluorination and the crude product was thus dried azeotropically and dissolved in acetonitrile and used in further testing without additional purification. A non-decay corrected radiochemical yield of 40% was achieved with a synthesis time of around 30 minutes. <sup>18</sup>F]NFSI produced this way was used to label allylsilanes and silyl enol ethers to create <sup>18</sup>F-labeled allylic

fluorides and  $\alpha$ -fluorinated ketones.  $[^{18}\text{F}]\text{NFSI}$  is tolerant to water but prefers anhydrous conditions for maximum reactivity.<sup>32</sup>  $[^{18}\text{F}]\text{NFSI}$  has been used in the  $^{18}\text{F}$ -labeling of the unprotected, branched aliphatic amino acids 4- $[^{18}\text{F}]$ fluoroleucine methyl ester, 5- $[^{18}\text{F}]$ fluorohomoleucine, 5- $[^{18}\text{F}]$ fluoro- $\beta$ -amino-homoleucine, 3- $[^{18}\text{F}]$ fluorovaline and 3- $[^{18}\text{F}]$ fluoroisoleucine<sup>33</sup>. In addition to these,  $[^{18}\text{F}]\text{NFSI}$  has also been used in the  $^{18}\text{F}$ -labeling of leucine containing unprotected peptides<sup>34</sup>.

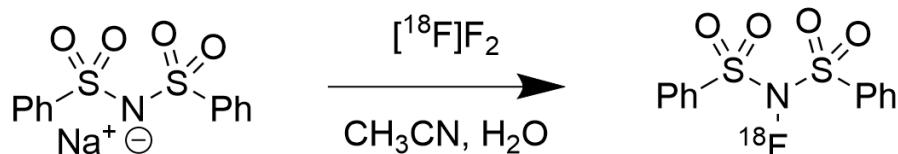


Figure 9: Synthesis of  $[^{18}\text{F}]\text{NFSI}$

### 1.2.9 N- $[^{18}\text{F}]$ Fluoropyridinium triflate

N- $[^{18}\text{F}]$ Fluoropyridinium triflate (fig. 10) is an electrophilic  $^{18}\text{F}$ -fluorinating reagent capable of fluorinating Grignard reagents and related carbanions and enolates.<sup>35</sup> It was first synthesized<sup>35</sup> by producing  $[^{18}\text{F}]\text{F}_2$  gas via the  $^{20}\text{Ne}(\text{d},\alpha)^{18}\text{F}$  nuclear reaction from neon gas that was mixed with 1%  $\text{F}_2$  gas. After production the created  $[^{18}\text{F}]\text{F}_2$  was bubbled through a solution of trimethylsilylpyridinium triflate in dry acetonitrile at  $-42\text{ }^\circ\text{C}$ . After the  $[^{18}\text{F}]\text{F}_2$  gas was passed through, the solution was evaporated to dryness and the remaining residue mixed with a small amount of diethyl ether. The diethyl ether was removed soon after addition by inverse filtration using a Schlenk tube equipped with a frit. After this the frit was backwashed using acetonitrile to recover the remaining N- $[^{18}\text{F}]$ fluoropyridinium triflate. Using this method a radiochemical yield of 46 % could be achieved.<sup>35</sup>

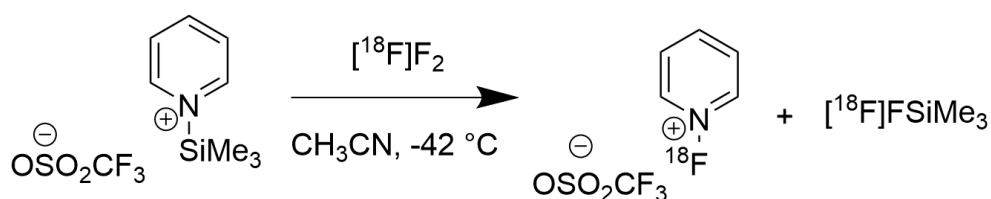


Figure 10: Synthesis of N- $[^{18}\text{F}]$ fluoropyridinium triflate

### 1.2.10 $[^{18}\text{F}]$ Selectfluor bis(triflate)

$[^{18}\text{F}]$ Selectfluor bis(triflate) (fig. 11) has in recent years become one of the premiere electrophilic  $^{18}\text{F}$ -fluorinating reagent not only due to its milder reactivity and improved regioselectivity when compared to  $[^{18}\text{F}]\text{F}_2$  gas but also due to a high level stability<sup>36,37</sup> and ability to fluorinate structures that other N-F type  $^{18}\text{F}$ -fluorinating reagents are not capable of<sup>38</sup>.  $[^{18}\text{F}]$ Selectfluor bis(triflate) was first synthesized<sup>38</sup> by producing  $[^{18}\text{F}]\text{F}_2$  gas via the  $^{18}\text{O}(\text{p},\text{n})^{18}\text{F}$  nuclear reaction using both 0.2% added carrier  $\text{F}_2$  method and also the Bergman and Solin method<sup>2</sup> of high voltage discharge that was

described previously in the  $[^{18}\text{F}]\text{F}_2$  section.  $[^{18}\text{F}]\text{Selectfluor bis(triflate)}$  was produced by bubbling the obtained  $[^{18}\text{F}]\text{F}_2$  through a 0.02 M solution of 1-chloromethyl-4-aza-1-azoniabicyclo[2.2.2]octane triflate and lithium triflate in acetonitrile at  $-10\text{ }^\circ\text{C}$ .  $[^{18}\text{F}]\text{F}_2$  gas produced both ways was tested and found to work, but the Bergman and Solin method<sup>2</sup> produced higher activities, 3-7 GBq when compared to 1-2 GBq using a carrier added method. After production the  $[^{18}\text{F}]\text{Selectfluor bis(triflate)}$  was dried by nitrogen gas flow at  $80^\circ\text{C}$  and afterwards the residue was dissolved in acetone. Analysis was done using radioHPLC,  $^{19}\text{F}$  NMR of decayed product and high-resolution electron impact mass spectrometry.  $[^{18}\text{F}]\text{Selectfluor bis(triflate)}$  produced using this method was used for the  $^{18}\text{F}$ -fluorination of silyl enol ether and Stannyl structures.<sup>38</sup> In a separate study by the same group arylboronic structures were also  $^{18}\text{F}$ -fluorinated to synthesize the radiotracer 6- $[^{18}\text{F}]\text{fluoro-L-DOPA}$ <sup>39</sup>.

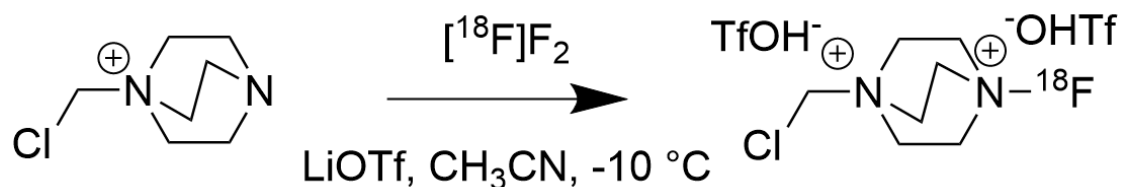


Figure 11: Synthesis of  $[^{18}\text{F}]\text{Selectfluor bis(triflate)}$

In addition to 6- $[^{18}\text{F}]\text{fluoro-L-DOPA}$ ,  $[^{18}\text{F}]\text{Selectfluor bis(triflate)}$  has been used in the  $^{18}\text{F}$ -labeling of the norepinephrine transporter tracer  $[^{18}\text{F}]\text{NS12137}$ <sup>40</sup> as well as  $[^{18}\text{F}]\text{F-DPA}$ <sup>41</sup> and 6- $[^{18}\text{F}]\text{Fluoro-marsanidine}$ <sup>42</sup>.

### 1.2.11 Transition metal electrophilic $^{18}\text{F}$ -fluorination reagents

The electrophilic  $^{18}\text{F}$ -fluorinating reagents described in the previous section were all metal free, but an electrophilic  $^{18}\text{F}$ -fluorinating reagent that utilizes palladium(IV) has also been developed. This reagent, benzo[*h*]quinolinyl (tetrapyrazolylborate) Pd(IV)  $[^{18}\text{F}]\text{fluoride trifluoromethanesulfonate}$ , works on the basis of performing an umpolung or polarity inversion of fluorine-18, transforming it from a nucleophilic form to an electrophilic form. This way it is possible produce fluorine-18 first in nucleophilic form to afford a greater starting molar activity, but also to have the great reactivity of electrophilic fluorine-18, combining the good sides of both methods while also mitigating the bad sides.<sup>43</sup>

Benzo[*h*]quinolinyl (tetrapyrazolylborate) Pd(IV)  $[^{18}\text{F}]\text{fluoride trifluoromethanesulfonate}$  is synthesized by first producing  $[^{18}\text{F}]\text{F}^-$  via the  $^{18}\text{O}(\text{p},\text{n})^{18}\text{F}$  nuclear reaction from  $^{18}\text{O}$  enriched water and loaded onto a solid phase extraction cartridge and washed with ultrapure water. After this the trapped  $[^{18}\text{F}]\text{F}^-$  is eluted out with a solution of  $\text{KHCO}_3$  in ultrapure water and diluted with acetone to

get a 4:1 mix of acetone and water. A solution of 18-crown-6 in acetonitrile is then added to this solution and the mixture is evaporated to dryness at 108 °C under a nitrogen gas stream. When dry, acetonitrile was added three times and each time the mixture was evaporated to dryness before another addition of acetonitrile. After this drying, the residue was cooled before benzo[*h*]quinoliny (tetrapyrzolyborate) Pd(IV) 4-picoline trifluoromethanesulfonate dissolved in acetone was added to it. The mixture was sonicated and then stirred at 23 °C for 10 minutes. After stirring the mixture was loaded via glass pipette onto another glass pipette that contained cotton and JandaJel™-polypyridine that had been suspended in acetone for 15 minutes. The reaction vessel was washed with acetone and the acetone used in the wash was added to the JandaJel™-polypyridine and the combined reaction and wash mixture pushed through the cotton and JandaJel™-polypyridine to a new vial. The previous reaction vial was washed again with acetone and also pushed through cotton and the JandaJel™-polypyridine and added with the rest.<sup>43</sup>

To use benzo[*h*]quinoliny (tetrapyrzolyborate) Pd(IV) [<sup>18</sup>F]fluoride trifluoromethanesulfonate in radiolabeling another palladium complex must be used, this time one that utilizes palladium(II) instead of palladium(IV). An example of such a compound and its reaction in radiolabeling with benzo[*h*]quinoliny (tetrapyrzolyborate) Pd(IV) [<sup>18</sup>F]fluoride trifluoromethanesulfonate is provided in figure 12.<sup>43</sup> The necessity of using two palladium complexes to make use of this umpolung method is a hinderance to it, any benefit that is gained using this method in simplifying the <sup>18</sup>F-labeling is lost in developing and synthesizing the palladium complexes needed for reactions with benzo[*h*]quinoliny (tetrapyrzolyborate) Pd(IV) [<sup>18</sup>F]fluoride trifluoromethanesulfonate. Nevertheless, these palladium reagents have been used to successfully <sup>18</sup>F-label the small drug-like molecules of paroxetine and a 5-HT<sub>2C</sub> agonist<sup>44</sup>.

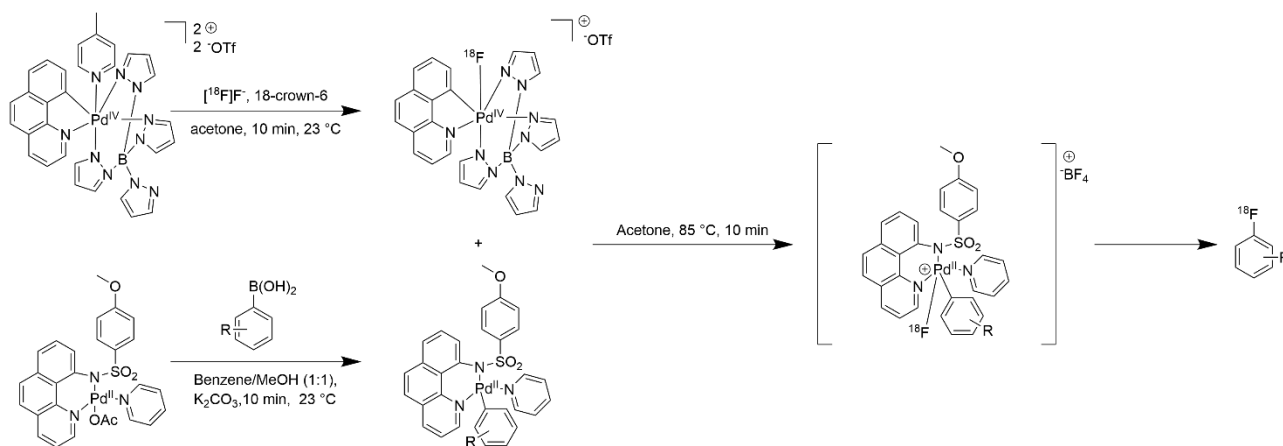


Figure 12: Typical synthesis of a <sup>18</sup>F-labeled compound using palladium complexes

### 1.2.12 [<sup>18</sup>F]Fluoro-benziodoxole

[<sup>18</sup>F]Fluoro-benziodoxole (fig. 13) is an electrophilic <sup>18</sup>F-fluorinating reagent that functions by the same principle as the previously described palladium(IV) reagent by performing an umpolung of the fluorine-18 from nucleophilic to electrophilic. The crucial advantage of [<sup>18</sup>F]fluoro-benziodoxole when compared to the palladium(IV) is the relative simplicity of its synthesis and use in radiolabeling. [<sup>18</sup>F]Fluoro-benziodoxole was first synthesized<sup>45</sup> by producing [<sup>18</sup>F]F<sup>-</sup> via the <sup>18</sup>O(p,n)<sup>18</sup>F nuclear reaction from oxygen-18 enriched water. [<sup>18</sup>F]F<sup>-</sup> was subsequently trapped in an anion exchange solid phase extraction cartridge and then eluted out by using a solution Bu<sub>4</sub>NHCO<sub>3</sub> in a 1:1 mixture of acetonitrile and water. After elution the activity was obtained as [<sup>18</sup>F]Bu<sub>4</sub>NF and after addition of acetonitrile it was dried for four minutes at 120 °C using a nitrogen gas flow. This drying was repeated two more times for two and three minutes respectively each time adding more acetonitrile before drying. After drying the residue was dissolved in dichloromethane and added to a vial containing 1-tosyloxy-3,3-dimethyl-1,3-dihydro-λ<sup>3</sup>-benzo[d][1,2]iodoxole and the mixture was stirred at room temperature for five minutes. After mixing the solution was dried under nitrogen gas flow for ten

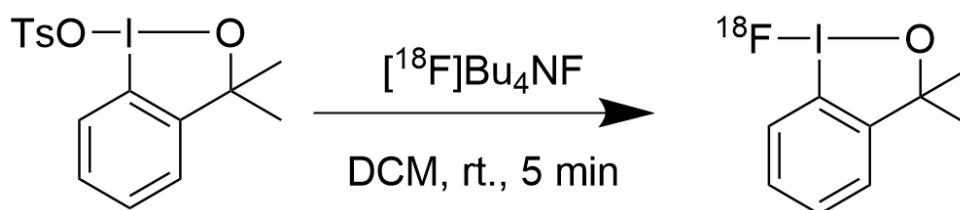


Figure 13: Synthesis of [<sup>18</sup>F]fluoro-benziodoxole

minutes. *n*-Hexane was added to the mixture before it was completely dry to ensure the formation of a solid. After drying more *n*-hexane was added to the solid and the mixture was stirred at 70 °C for one minute. After this the mixture was extracted using a syringe and filtered through a 1 mL IST Phase Separator®. The [<sup>18</sup>F]fluoro-benziodoxole produced this way was used in the radiolabeling of various *o*-styrylamide structures to create different fluorobenzoxazepines.<sup>45</sup>

[<sup>18</sup>F]Fluoro-benziodoxole has not been used in the radiolabeling of many structures. The only other reported radiosynthesis that uses [<sup>18</sup>F]fluoro-benziodoxole, was to radiolabel diazoketone structures via a rhodium mediated method<sup>46</sup>. And so one of the aims of this work was to test the potential use of [<sup>18</sup>F]fluoro-benziodoxole in the synthesis of the radiotracer [<sup>18</sup>F]UCB-J to see whether [<sup>18</sup>F]Fluoro-benziodoxole could see larger use in the future of electrophilic <sup>18</sup>F-chemistry.

### 1.3 UCB-J

UCB-J is a radiotracer that is used for the imaging of the synaptic vesicle glycoprotein 2A density and as mentioned previously the aim of this work was to synthesize  $^{18}\text{F}$ -labeled UCB-J using the electrophilic  $^{18}\text{F}$ -fluorinating reagent  $[\text{}^{18}\text{F}]$ fluoro-benziodoxole. UCB-J as a radiotracer has been previously used as  $^{11}\text{C}$ -labeled  $[\text{}^{11}\text{C}]$ UCB-J<sup>47</sup>, however due to the beneficial qualities of fluorine-18 such as a longer half-life and good energy resolution, a  $^{18}\text{F}$ -labeled version is of interest. Previous attempts to label UCB-J using nucleophilic fluorine-18 have not been successful or have resulted in low radiochemical yields<sup>48</sup>. However a working electrophilic method has been developed to  $^{18}\text{F}$ -radiolabel UCB-J utilizing the electrophilic  $^{18}\text{F}$ -fluorinating reagent  $[\text{}^{18}\text{F}]$ Selectfluor bis(triflate)<sup>49</sup>. The advantage of a  $[\text{}^{18}\text{F}]$ fluoro-benziodoxole mediated method over this  $[\text{}^{18}\text{F}]$ Selectfluor bis(triflate) method would be the ability to achieve higher molar activities due to the ability of  $[\text{}^{18}\text{F}]$ fluoro-benziodoxole to perform an umpolung of fluorine-18 without the need for isotopic dilution with fluorine-19. In addition to this, the potential for a wider use of electrophilic  $^{18}\text{F}$ -labeling as  $[\text{}^{18}\text{F}]$ fluoro-benziodoxole could allow for already existing facilities that employ mainly nucleophilic methods to adopt it in use and employ electrophilic synthesis.

## 2 Experiment

### 2.1 Aims of the work

The aim of this work was to study the viability of producing [ $^{18}\text{F}$ ]UCB-J using [ $^{18}\text{F}$ ]fluoro-benziodoxole as a direct fluorinating reagent. For this purpose four different [ $^{18}\text{F}$ ]fluoro-benziodoxole precursors were synthesized to find the most suitable one for the production of [ $^{18}\text{F}$ ]UCB-J. In addition to testing the viability of producing [ $^{18}\text{F}$ ]UCB-J via [ $^{18}\text{F}$ ]fluoro-benziodoxole the other aim of this work was to study the metabolism of [ $^{18}\text{F}$ ]UCB-J in rats.

### 2.2 Synthesis of [ $^{18}\text{F}$ ]fluoro-benziodoxole precursors

The goal was to synthesize four different hypervalent iodine compounds using the method of Koser et al.<sup>50</sup> as a basis. The compounds are presented in figure 14: 1-tosyloxy-3,3-dimethyl-1,3-dihydro- $\lambda^3$ -benzo[d][1,2]iodoxole (1), 3,3-dimethyl-1- $\lambda^3$ -benzo[d][1,2]iodaoxol-1(3H)-yl 2,2,2-trifluoroacetate (2), 3,3-dimethyl-1- $\lambda^3$ -benzo[d][1,2]iodaoxol-1(3H)-yl acetate (3) and 1-((chloromethyl)-4-diazabicyclo[2.2.2]octane-1,4-diiumoxy)carbonyl)-1,4-diazabicyclo[2.2.2]octane-1,4-diium (4).

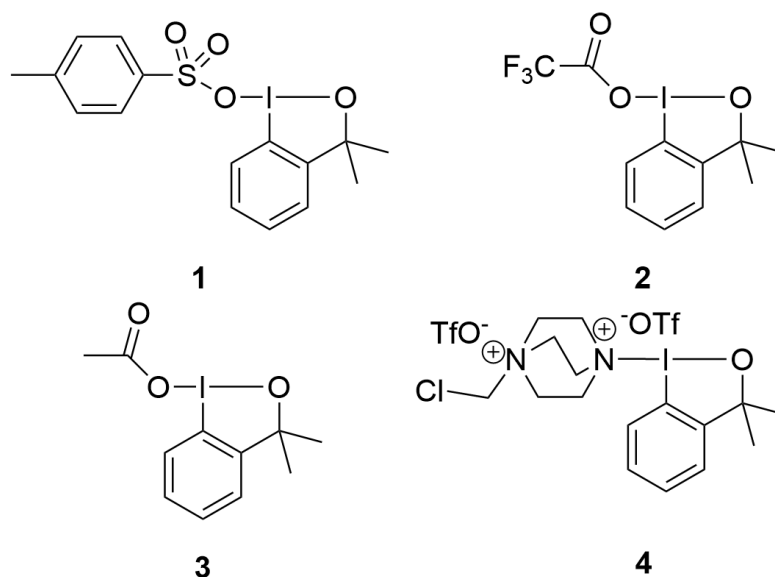


Figure 14: [ $^{18}\text{F}$ ]Fluoro-benziodoxole precursors 1, 2, 3 and 4

Compound 1 was synthesized using the method of Koser et al.<sup>50</sup> with the amounts used by Geary et al.<sup>51</sup> Thus 0.6 mL of 2-iodophenylpropan-2-ol (3.68 mmol) and 1.58 g of hydroxy(tosyloxy)iodo]benzene (4.03 mmol) were added to 19 mL of DCM and the solution was stirred at room temperature overnight. The resulting product was evaporated to dryness in a rotary

evaporator to give a solid product, which was washed three times with 10 mL of hexane. An amount of 0.95 g (2.19 mmol) of product was obtained with a yield of 59%. The product was analyzed by NMR.

Compound **2** was synthesized by mixing 0.15 mL (0.95 mmol) of 2-iodophenylpropan-2-ol and 420 mg (0.98 mmol) of PIFA in 19 mL of DCM. The solution was stirred overnight, after which it was evaporated to dryness in a rotary evaporator and was washed three times with 10 mL of hexane. An amount of 291 mg (0.78 mmol) of product was obtained, the yield being 81%. The product was analyzed by NMR.

The synthesis of Compound **3** was attempted in the same way as **2** by adding 0.15 mL (0.95 mmol) of 2-iodophenylpropan-2-ol and 302 mg (0.94 mmol) of PIDA to 19 mL of DCM. The solution was stirred overnight and dried on a rotary evaporator. From this reaction 229 mg of recovered solid compound was obtained and this was analyzed by NMR.

Compound **4** was synthesized by mixing together 35.5 mg (0.079 mmol) of bis(4-(chloromethyl)-1,4-diazabicyclo[2.2.2]octan-1,4-diium-1-yl)iodate(I) and 6  $\mu$ L (0.94 mmol) of 2-iodophenylpropane -2-ol together with 1 mL of DCM and the solution was allowed to stir at room temperature overnight. An amount of 19.3 mg (0.046 mmol) of the product was obtained with a yield of 54%. The product was analyzed by NMR.

### 2.3 Synthesis of [ $^{18}\text{F}$ ]UCB-J

Synthesis of [ $^{18}\text{F}$ ]UCB-J was performed using all four [ $^{18}\text{F}$ ]fluoro-benziodoxole precursors. Syntheses were done using a synthesis device following the general methodology published by González et al. and products were analyzed using radioHPLC. The general synthesis scheme is presented in figure 15.

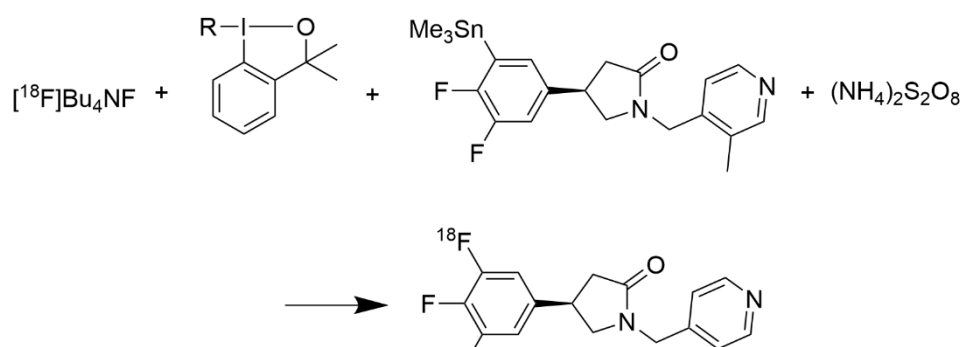


Figure 15: General synthesis scheme of [ $^{18}\text{F}$ ]UCB-J where R = different precursor substitutes

### 2.3.1 [<sup>18</sup>F]Tetrabutylammonium fluoride production

Synthesis of [<sup>18</sup>F]UCB-J was first done using **1** as the [<sup>18</sup>F]fluoro-benziodoxole precursor. [<sup>18</sup>F]Tetrabutylammonium fluoride was synthesized by first preparing a Sep-Pak Plus Light QMA Cartridge by wetting it with 10 mL of water and then cyclotron produced [<sup>18</sup>F]F<sup>-</sup> in 10 mL of water was trapped in it. After trapping the cartridge was washed with 10 mL of acetonitrile and after washing the trapped [<sup>18</sup>F]F<sup>-</sup> was eluted out by 500 μL of a 50:50 mixture of acetonitrile and 0.075 M tetrabutylammonium carbonate. This elution was dried three times azeotropically by adding 200 μL of acetonitrile each time. After drying the formed product was dissolved in 700 μL of dichloromethane.

### 2.3.2 [<sup>18</sup>F]UCB-J production

The produced [<sup>18</sup>F]tetrabutylammonium fluoride was then added to 4.9 mg of tosylate precursor and stirred at room temperature for five minutes. After stirring, 200 μL of the mixture was portioned off and the remaining 500 μL was evaporated to dryness and the resulting solid was redissolved in 500 μL of hexane and stirred for five minutes. This hexane solution was then divided in two 200 μL portions. The rest of the reagents were added to each portion in amounts presented in table 1

Table 1: Reagents for [<sup>18</sup>F]UCB-J synthesis using **1** as [<sup>18</sup>F]fluoro-benziodoxole precursor

Denomination	Solvent (200 μL)	Me <sub>3</sub> Sn-UCB-J (mg)	(NH <sub>4</sub> ) <sub>2</sub> S <sub>2</sub> O <sub>8</sub> (mg)
Reaction 1	DCM	0.8	3.7
Reaction 2	Hexane	1.1	3.4
Reaction 3	Hexane	1.0	3.0

Reactions 1 and 2 were stirred at 70°C for 10 minutes before being analyzed by radioHPLC. Reaction 3 was evaporated to dryness under argon gas flow for five minutes and then dissolved in 400 μL of acetone-*d*<sub>6</sub> and stirred at 70°C for 10 minutes before being analyzed by radioHPLC.

The [<sup>18</sup>F]tetrabutylammonium fluoride was prepared as described in the previous section for reactions 4 and 5. The dry solid [<sup>18</sup>F]tetrabutylammonium fluoride was dissolved in 750 μL of acetone-*d*<sub>6</sub>. From this solution two stocks of 250 μL were then taken for further reactions. The rest of the reagents were added in the amounts presented in table 2.

Table 2: Reagents for synthesis of [<sup>18</sup>F]UCB-J using **1** and **2** as [<sup>18</sup>F]fluoro-benziodoxole precursor

Denomination	[ <sup>18</sup> F]Fluoro-benziodoxole precursor	Me <sub>3</sub> Sn-UCB-J (mg)	(NH <sub>4</sub> ) <sub>2</sub> S <sub>2</sub> O <sub>8</sub> (mg)
Reaction 4	2.4 mg ( <b>1</b> )	0.88	5.2
Reaction 5	4.14 mg ( <b>fluoro-benziodoxole</b> )	1.03	4.09

Both reactions 4 and 5 were then stirred at 60 °C for 10 minutes before being analyzed by radioHPLC.

The [<sup>18</sup>F]tetrabutylammonium fluoride was prepared as described in the previous section for reactions 6-9. The dry solid [<sup>18</sup>F]tetrabutylammonium fluoride was then dissolved in 1.5 mL of acetone-*d*<sub>6</sub>. From this solution four stocks of 250 μL were then taken for further reactions. The rest of the reagents were added in the amounts presented in table 3.

Table 3: Reagents for synthesis of [<sup>18</sup>F]UCB-J using **2** and **4** as [<sup>18</sup>F]fluoro-benziodoxole precursors

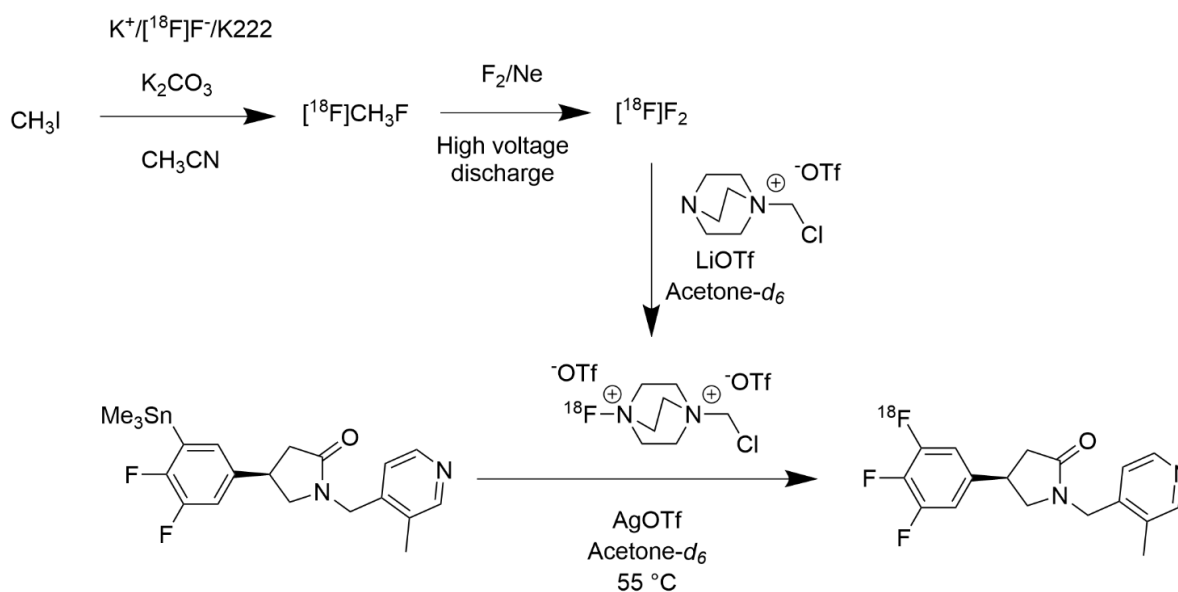
Denomination	[ <sup>18</sup> F]Fluoro-benziodoxole precursor	Me <sub>3</sub> Sn-UCB-J (mg)	(NH <sub>4</sub> ) <sub>2</sub> S <sub>2</sub> O <sub>8</sub> (mg)
Reaction 6	3.09 mg ( <b>2</b> )	0.78	1.19
Reaction 7	1.99 mg ( <b>4</b> )	0.83	0.96
Reaction 8	1.92 mg ( <b>4</b> )	0.75	1.03

All reactions were stirred at 70 °C for 10 minutes before being analysed by radioHPLC.

## 2.4 [<sup>18</sup>F]UCB-J radiometabolism in rats

### 2.4.1 [<sup>18</sup>F]UCB-J synthesis

[<sup>18</sup>F]UCB-J for the radiometabolism study was produced using the method published by Keller et al.<sup>49</sup> presented in figure 16 and purified by preparatory HPLC.

Figure 16: Synthesis of [<sup>18</sup>F]UCB-J utilizing [<sup>18</sup>F]Selectfluor bis(triflate)

The study was approved by the Regional State Administrative Agency for Southern Finland (license number ESAVI-33741-2019\_muutospäätös-011119\_ESAVI-16273-2019). The animal studies were performed on three 68-day old female Sprague Dawley rats of the TgF344-AD rat model. The animals were group-housed under standard conditions (temperature  $21 \pm 3$  °C, humidity  $55 \pm 15$  %, lights on from 06:00 until 18:00) at the Central Animal Laboratory, University of Turku, Turku, Finland.

The three rats were injected with [ $^{18}\text{F}$ ]UCB-J and sacrificed one hour after injection. After sacrifice biodistribution of radioactivity was studied from animal blood, plasma, erythrocytes, tail, brain, liver and urine. This was done by weighing each sample organ whole except the liver from where only a sample was taken from the organ and weighed and measuring radioactivity from each organ. Results are reported as percentage of injected dose per gram (%ID/g) after decay correction.

#### 2.4.2 [ $^{18}\text{F}$ ]UCB-J radiometabolism studies

Radiometabolism of the injected [ $^{18}\text{F}$ ]UCB-J was studied by taking samples from the plasma, brain, liver and urine of the animals that were sacrificed one hour after injection. The test animals were injected with  $9.24 \pm 3.22$  MBq of activity. The samples were analyzed by using normal and reverse phase radioTLC and radioHPLC.

For the radioTLC analysis the blood samples were taken in Li-heparin tubes and diluted with acetonitrile to reach a 1:2 plasma acetonitrile solution in order to precipitate proteins present in the plasma. The blood samples were then centrifuged for 90 seconds at 14100 g and a sample of the supernatant was applied to aluminum backed silica gel 60 RP-18 1.0559.0001 TLC plates for reverse phase TLC and silica gel 60 1.0553.0001 TLC plates for normal phase TLC (Merck Millipore, Darmstadt, Germany). The urine samples were diluted also using acetonitrile to get a 1:3 urine acetonitrile solution and also centrifuged for 90 seconds at 14 100 g and the sample of the supernatant was applied to the TLC plates. The brain samples were homogenized using a 1:1 solution of water and methanol and then centrifuged for 3 minutes at 14100 g after which a sample of the resulting supernatant was applied to the TLC plates. Liver samples were also homogenized using a 1:1 solution of water and methanol and centrifuged for 3 minutes at 14 100 g before the resulting supernatant was sampled to the TLC plates. The amounts of sample applied to the TLC plates are presented in table 4.

Table 4: Applied sample amounts for radioTLC, where RP = reverse phase, NP = normal phase and Std = standard

Animal	RP Std (µL)	RP Plasma (µL)	RP Brain (µL)	RP Liver (µL)	RP Urine (µL)	NP Std (µL)	NP Plasma (µL)	NP Brain (µL)	NP Liver (µL)	NP Urine (µL)
Rat 1	2	12	18	18	1	3	18	18	18	1
Rat 2	2	12	18	12	1	2	18	18	12	0.5
Rat 3	2	12	18	12	0.5	2	18	18	12	0.5

The eluent used for reverse phase radioTLC was 75:25 mixture of acetonitrile and 0.2 M ammonium fluoride. For reverse phase radioTLC the used eluent was a 5:1 mixture of dichloromethane and methanol with 0.1 % of trifluoroacetic acid added in. The TLC plates were eluted for 6 cm with an average elution time of around 5 minutes. After elution the TLC plates were pressed for two fluorine-18 half-lives against imaging plates (Fuji BAS Imaging Plate TR2025, Fuji Photo Film Co., Ltd., Tokyo, Japan) to create an autoradiography image of the TLC plates. The imaging plates were read using BAS-5000 (Fuji, Japan) imaging system with a resolution of 50 µm and the created images were analyzed with TINA software (version 2.10 g, Raytest, Isotopenmessgeräte, GmbH, Straubenhardt, Germany).

In addition to radioTLC the samples from plasma, brain, liver and urine of the test animals were also analyzed using radioHPLC. Samples from the plasma, brain and urine were analyzed from each test animal but only one liver sample from a single animal was analyzed by radioHPLC. Injected amounts of homogenized sample are presented in table 5. The used eluent was a 5:1 mixture of water and 35:65 acetonitrile:water.

Table 5: Amount of injected sample for radioHPLC analysis

Animal	Sample	Amount injected (µL)
Rat 1	Plasma	500
Rat 1	Brain	80
Rat 1	Urine	10
Rat 2	Plasma	400
Rat 2	Brain	70
Rat 2	Urine	5
Rat 3	Plasma	750
Rat 3	Brain	90
Rat 3	Urine	6
Rat 1	Liver	50

### 3 Results

#### 3.1.1 Synthesis of [<sup>18</sup>F]Fluoro-benziiodoxole precursors

The yields for the [<sup>18</sup>F]fluoro-benziiodoxole precursor compounds **1-4** is presented in table 6. The [<sup>18</sup>F]fluoro-benziiodoxole precursors were characterized using <sup>1</sup>H-NMR. The yield for the synthesis was good with all being over 50% and even reaching 80%.

Table 4: Yields for [<sup>18</sup>F]fluoro-benziiodoxole precursor compounds **1-4**

[ <sup>18</sup> F]Fluoro-benziiodoxole precursor	Yield
<b>1</b>	59 %
<b>2</b>	81 %
<b>3</b>	0 %
<b>4</b>	54 %

The <sup>1</sup>H-NMR spectrum for compound **1** was:  $\delta_{\text{H}}$  (500 MHz, DMSO) 1.57 (6H, s, 2 x CH<sub>3</sub>), 2.29 (3H, s, CH<sub>3</sub>), 7.11 (2H, d, ArH), 7.45 (1H, d, ArH), 7.47 (2H, d, ArH), 7.60 (1H, d, ArH), 7.62 (1H, s, ArH), 7.66 (1H, t, ArH).

The <sup>1</sup>H-NMR spectrum for compound **2** was:  $\delta_{\text{H}}$  (500 MHz, CDCl<sub>3</sub>) 1.60 (6H, s, 2 x CH<sub>3</sub>), 7.21 (1H, dd, ArH), 7.52 (1H, dt, ArH), 7.58 (1H, dt, ArH), 7.74 (1H, dd, ArH).

The <sup>1</sup>H-NMR spectrum for solid compounds recovered during the synthesis of compound **3** was:  $\delta_{\text{H}}$  (500 MHz, CDCl<sub>3</sub>) 2.03 (3H, s, CH<sub>3</sub>), 7.28 (1H, s, ArH), 7.50 (1H, t, ArH), 7.60 (1H, t, ArH), 8.10 (1H, d, ArH). This corresponds to the NMR for the PIDA starting material.

The <sup>1</sup>H-NMR spectrum for compound **4** was:  $\delta_{\text{H}}$  (500 MHz, DMSO) 1.61 (6H, s, 2 x CH<sub>3</sub>), 3.21 (44H, t, CH<sub>2</sub>), 3.45 (47H, t, CH<sub>2</sub>), 5.33 (14H, s), 5.7 (2H, s, DCM), 6.90 (1H, t, ArH), 7.35 (1H, t, ArH), 7.75 (1H, d, ArH), 7.92, (1H, d, ArH). ). The spectrum images are included in attachments as attachments 1-4.

The spectra for compounds **1** and **2** show the expected number of protons and within the expected ranges and can be identified as the desired products. The spectrum for the recovered solid from the synthesis of compound **3** is missing six protons corresponding to the two methyl groups in the base hypervalent iodine structure that should be visible at around 1.60 ppm if this solid was compound **3**, this means that the recovered solid is just the unreacted starting material PIDA, and the synthesis failed. Compound **4** has a messy spectrum with wide peaks, indicating an impure product, but it has

the expected peaks in the expected ranges, although showing an incorrect number of protons in the case of the peaks at 3.21 ppm and 3.45 ppm.

### 3.1.2 [ $^{18}\text{F}$ ]UCB-J synthesis via [ $^{18}\text{F}$ ]fluoro-benziodoxole

The radioHPLC chromatogram results for the reactions 1-8 are presented here. For each reaction product an ultraviolet (UV) and radioactivity (RA) chromatogram are presented and when compared to the reference chromatogram the result of the reaction can be determined. The UV chromatogram is shown in black and the RA chromatogram in red in each figure. The reference chromatogram (fig. 17) was created by injecting 17  $\mu\text{L}$  of non-labelled UCB-J with a mass concentration of 0.1  $\text{mg ml}^{-1}$ . For a successful synthesis of [ $^{18}\text{F}$ ]UCB-J a peak matching the main peak from the reference chromatogram should be present in both the ultraviolet and radioactivity chromatogram.

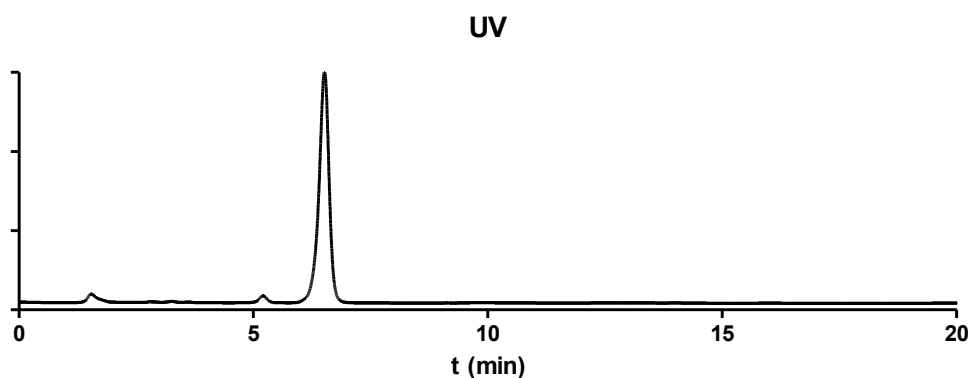


Figure 17: UCB-J reference chromatogram

In figure 17 three we can see a major peak at around 6.5 minutes corresponding to UCB-J, alignment with this peak is desired in the product chromatograms. The radioHPLC results for reaction 1 are presented in figure 18, where we can see that a corresponding peak is not present in the UV chromatogram. A slightly earlier peak corresponding to a hydride of  $\text{SnMe}_3\text{-UCB-J}$ , which does not have a corresponding radioactivity peak as it is not labelled with fluorine-18 but rather with a hydrogen.

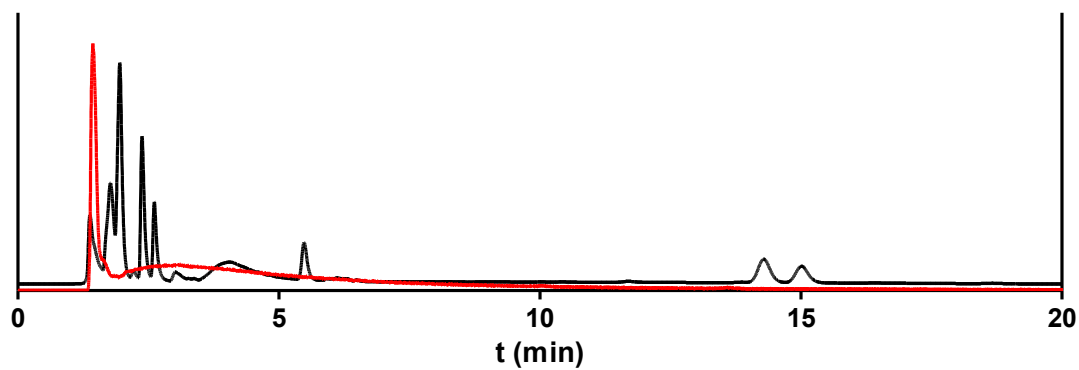


Figure 18: radioHPLC chromatogram for Reaction 1

The radioHPLC results for reaction 2 are presented in figure 19 where we can see that both the UV and radioactivity chromatograms are messy with wide peaks, an undesirable result as we cannot distinguish a peak corresponding to the reference from either chromatogram.

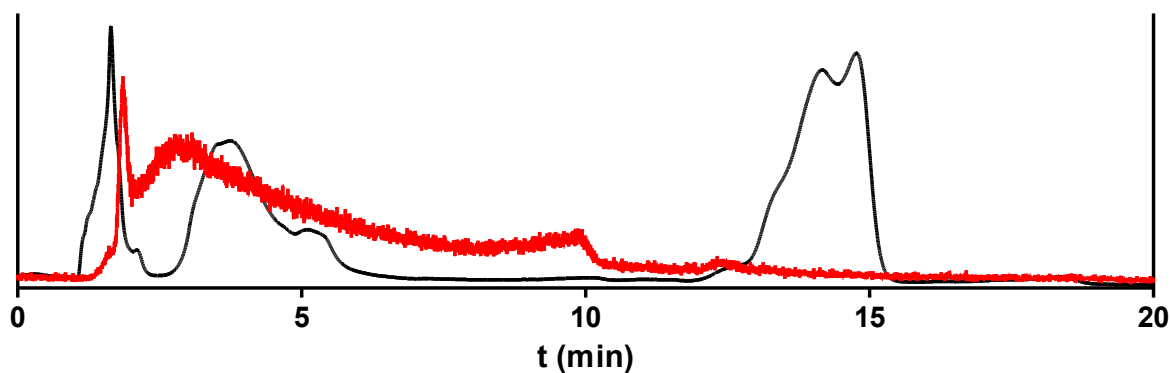


Figure 19: radioHPLC chromatogram for Reaction 2

The radioHPLC results for reaction 3 are presented in figure 20 where we can see an earlier peak corresponding to the hydride of  $\text{SnMe}_3\text{-UCB-J}$  but no peak corresponding to the reference gram in either UV or radioactivity chromatogram.

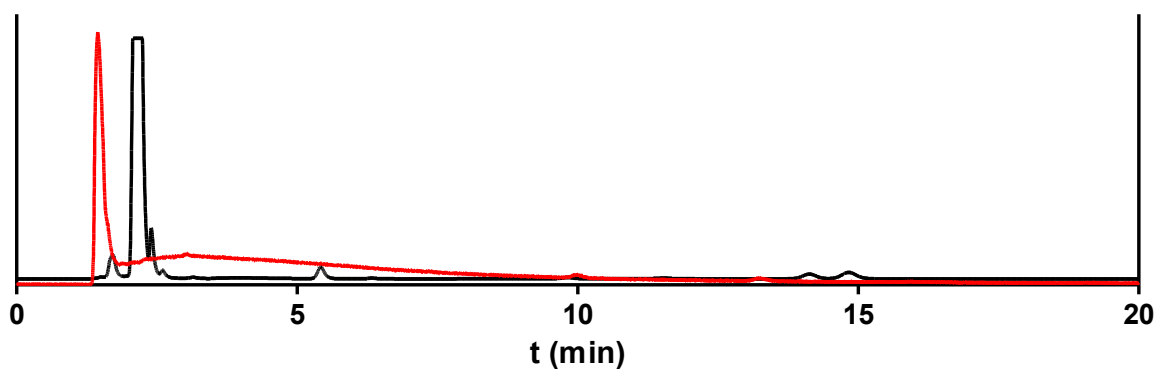


Figure 20: radioHPLC chromatogram for Reaction 3

The radioHPLC results for reaction 4 are presented in figure 21 where again there is no peak corresponding to the reference, only for the hydride of SnMe<sub>3</sub>-UCB-J.

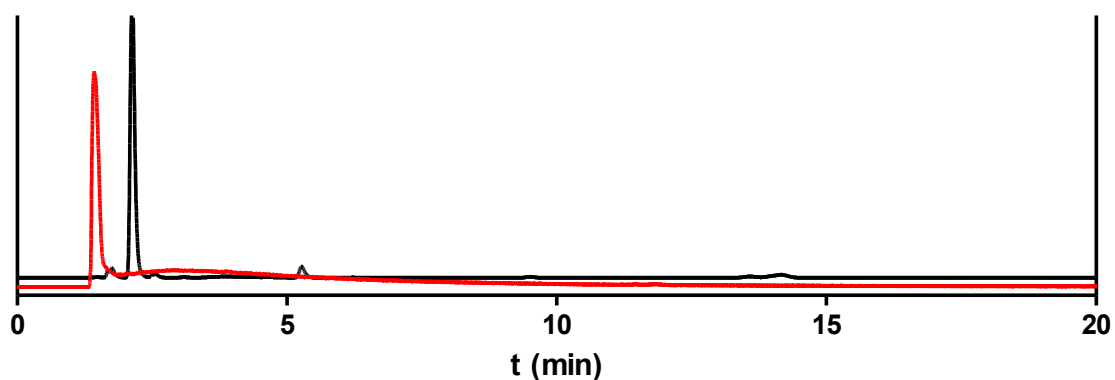


Figure 21: radioHPLC chromatogram for Reaction 4

The radioHPLC results for reaction 5 are presented in figure 22 where no peak matching the reference is seen, only the SnMe<sub>3</sub>-UCB-J hydride peak.

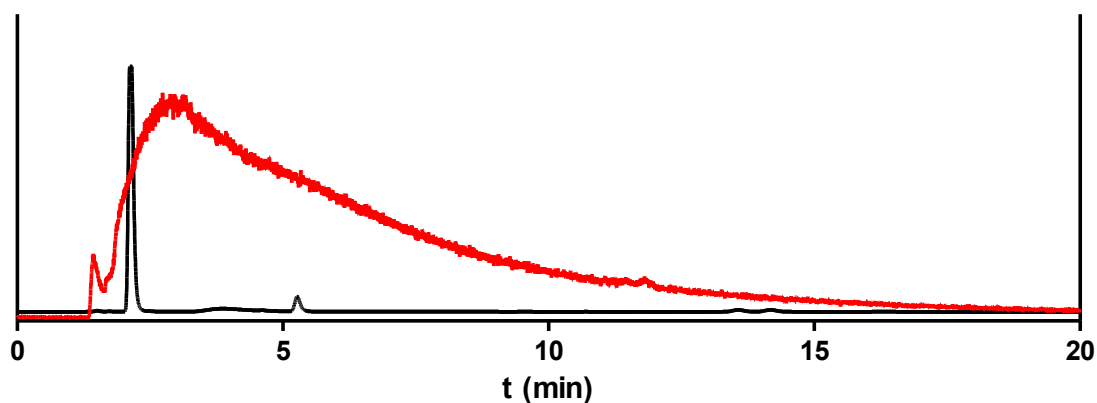


Figure 22: radioHPLC chromatogram for Reaction 5

The radioHPLC results for reaction 6 are presented in figure 23, where no peak matching the reference can be seen.

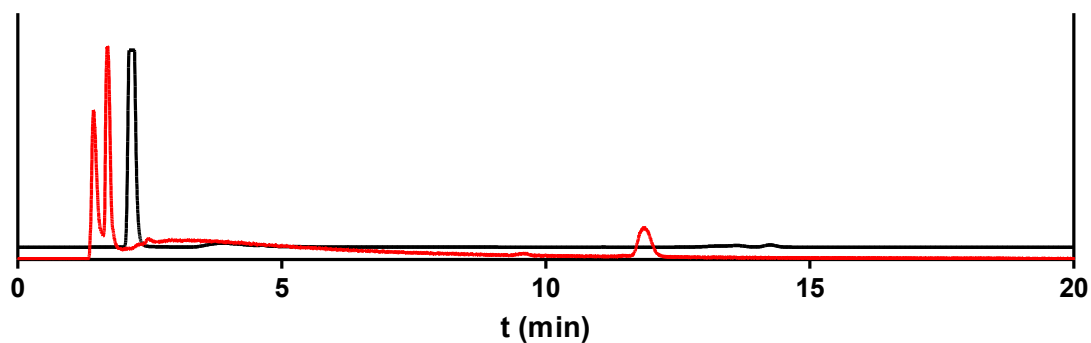


Figure 23: radioHPLC chromatogram for Reaction 6

The radioHPLC results for reaction 7 are presented in figure 24, where no peak corresponding to the reference can be seen but a peak corresponding to the hydride of SnMe<sub>3</sub>-UCB-J is visible.

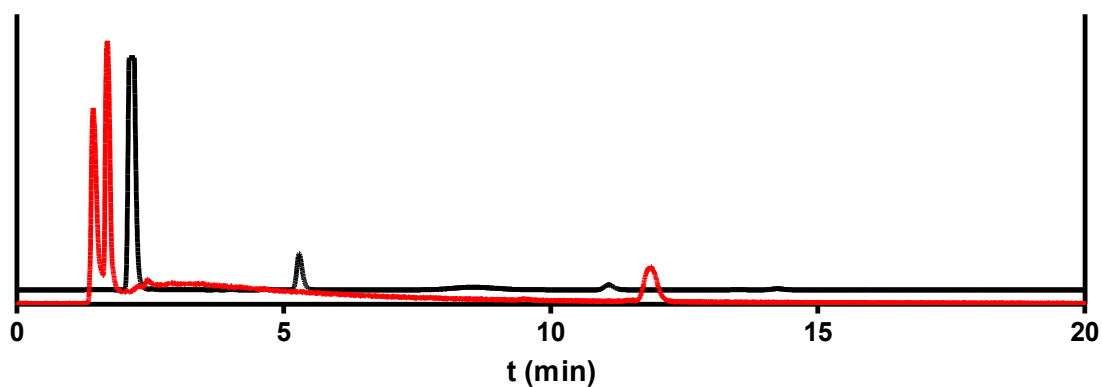


Figure 24: radioHPLC chromatogram for Reaction 7

The radioHPLC results for reaction 8 are presented in figure 25 where no peak corresponding to the reference is visible only a peak corresponding to the hydride of SnMe<sub>3</sub>-UCB-J can be seen.

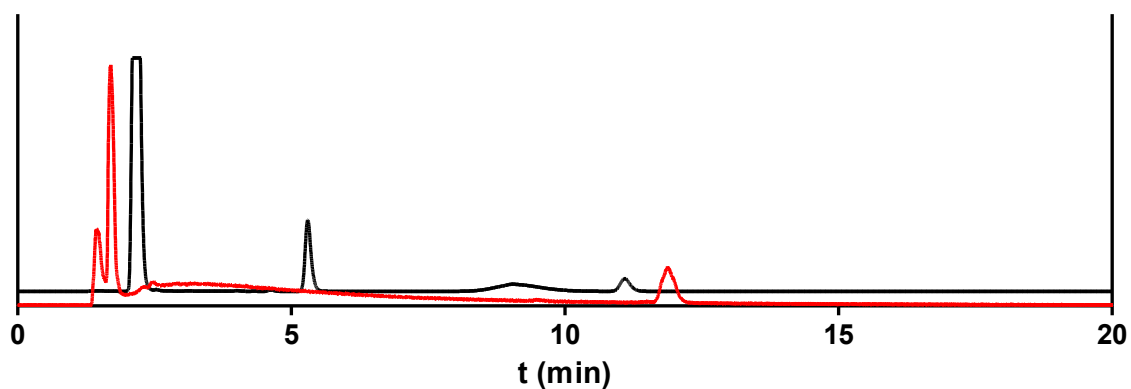


Figure 25: radioHPLC chromatogram for Reaction 8

No produced [ $^{18}\text{F}$ ]UCB-J could be detected in any of the radioHPLC chromatograms. Based on this it can be concluded that the [ $^{18}\text{F}$ ]fluoro-benziodoxole method does not work for [ $^{18}\text{F}$ ]UCB-J production.

### 3.1.3 Selectfluor synthesis of [ $^{18}\text{F}$ ]UCB-J for metabolism studies

The [ $^{18}\text{F}$ ]UCB-J used in the metabolism studies was produced via a selectfluor mediated method due to the uncertainty of whether the [ $^{18}\text{F}$ ]fluoro-benziodoxole method would work. For this reason, a method that is known to work<sup>49</sup> was chosen.

### 3.1.4 Biodistribution of injected activity

The results of the biodistribution of injected activity study are reported in figure 26 per tissue for each test animal using the unit percentage of injected dose per gram of tissue (%ID/g). From these results we can determine the distribution of [ $^{18}\text{F}$ ]UCB-J in the test animals one hour after injection. From figure 27 it can be seen that most of the activity and therefore the injected [ $^{18}\text{F}$ ]UCB-J is concentrated in the urine, liver, cortex and brain of the test animals with only minimal amounts in the blood, plasma and erythrocytes. The tail of the test animals are included as it was the injection site for the [ $^{18}\text{F}$ ]UCB-J.

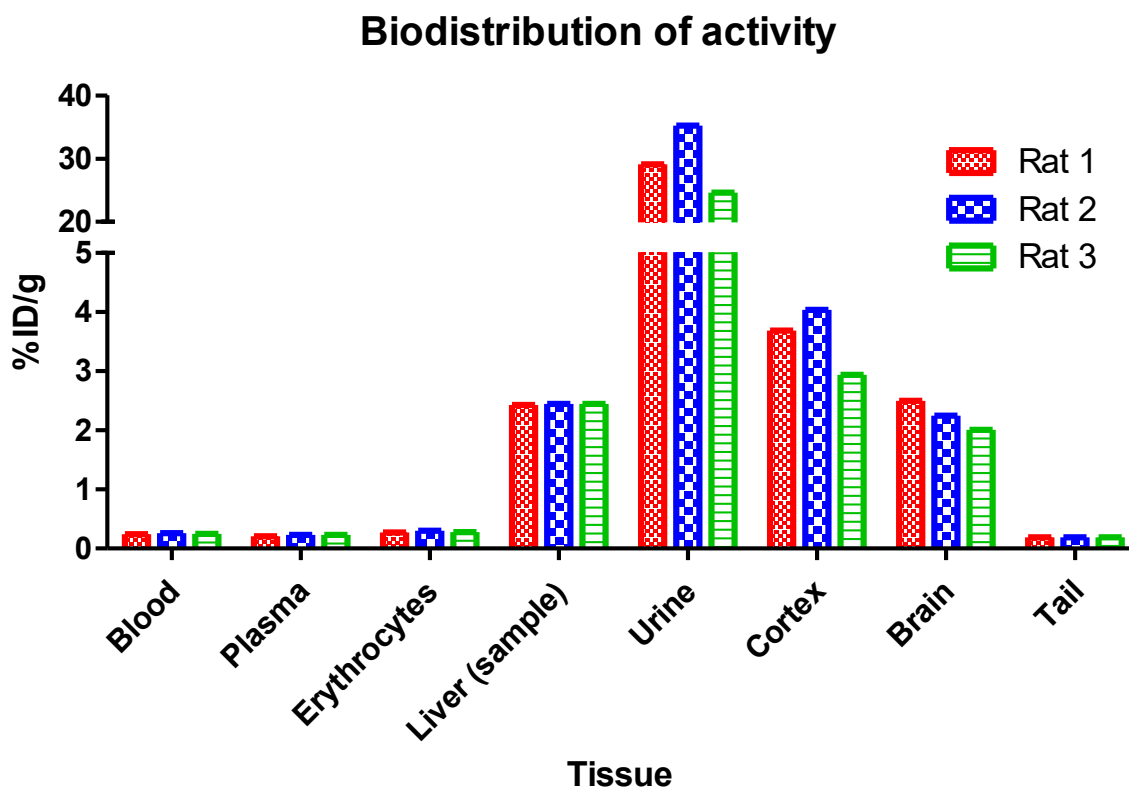


Figure 26: Percentage of injected activity per gram of tissue for each studied organ

These results are within expectations, most of the activity is present in the urine of the animals as the injected [ $^{18}\text{F}$ ]UCB-J has been metabolized and become ready for secretion. The liver has activity present as it is one of the body's main organs for metabolizing compounds and the injected [ $^{18}\text{F}$ ]UCB-J would gather there before being secreted. The brain and cortex of the animals has activity present as they contain the binding sites for [ $^{18}\text{F}$ ]UCB-J is meant to target, the synaptic vesicle glycoprotein 2A. The blood, plasma and erythrocytes contain small amounts of activity as the blood veins are transporting the activity and the [ $^{18}\text{F}$ ]UCB-J has no reason to concentrate in them. The same goes for the tail which is the injection site, as the injected [ $^{18}\text{F}$ ]UCB-J has been transported away for the body to process.

### 3.1.5 Radiometabolism study

The results of the radioTLC are presented in figures 27, 28 and 29, where the chromatograms of the radioTLC plates are overlaid with autoradiography images of the TLC plates. From these figures the degree of radiometabolism from each sample can be determined by comparing it with the reference [ $^{18}\text{F}$ ]UCB-J chromatogram. From the elution time we can see that the radiometabolites interacted more with the reverse phase TLC plates as the peaks in those chromatograms are seen earlier than in the normal phase chromatogram, from this we can deduce that the radiometabolites are

more polar than non-polar. The larger the peak for each sample that is aligned with the reference peak, the more the sample has non-metabolized [ $^{18}\text{F}$ ]UCB-J. We can see that the brain and liver samples have in general the largest amount of non-metabolized [ $^{18}\text{F}$ ]UCB-J with the plasma samples having some amount of non-metabolized [ $^{18}\text{F}$ ]UCB-J and the urine samples containing almost no non-metabolized [ $^{18}\text{F}$ ]UCB-J. The brain samples containing non-metabolized [ $^{18}\text{F}$ ]UCB-J is a good sign as [ $^{18}\text{F}$ ]UCB-J images the synaptic vesicle glycoprotein 2A in the brain and a large degree of metabolism would result in a lower resolution PET image. The liver containing non-metabolized [ $^{18}\text{F}$ ]UCB-J is also to be expected as [ $^{18}\text{F}$ ]UCB-J would be concentrated there for metabolism. The plasma sample has a small amount of non-metabolized [ $^{18}\text{F}$ ]UCB-J present as the blood veins are used for transporting both the metabolized and non-metabolized [ $^{18}\text{F}$ ]UCB-J to their destinations. The urine sample has almost no non-metabolized [ $^{18}\text{F}$ ]UCB-J because the metabolized [ $^{18}\text{F}$ ]UCB-J has been concentrated in the urine for excretion.

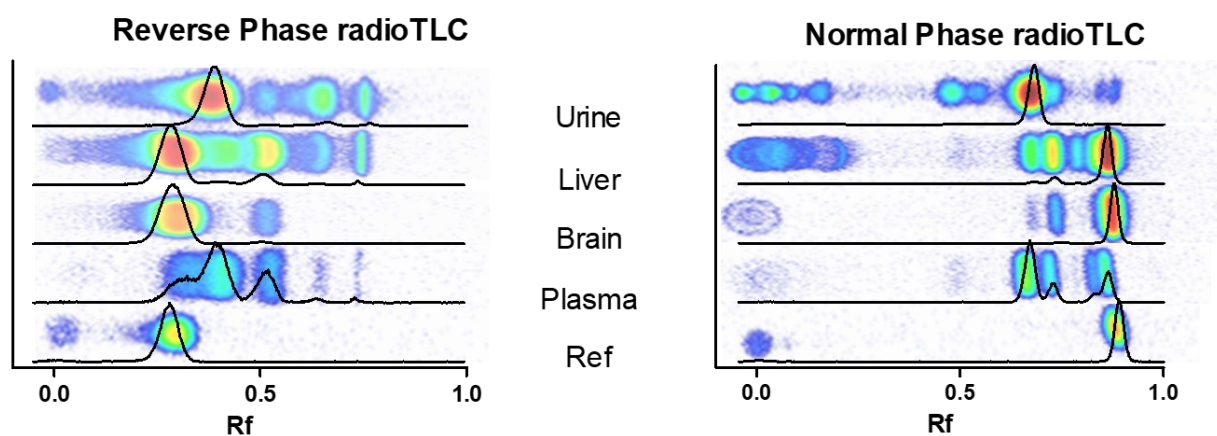


Figure 27: radioTLC chromatograms overlaid with autoradiography of TLC plates taken from rat 1

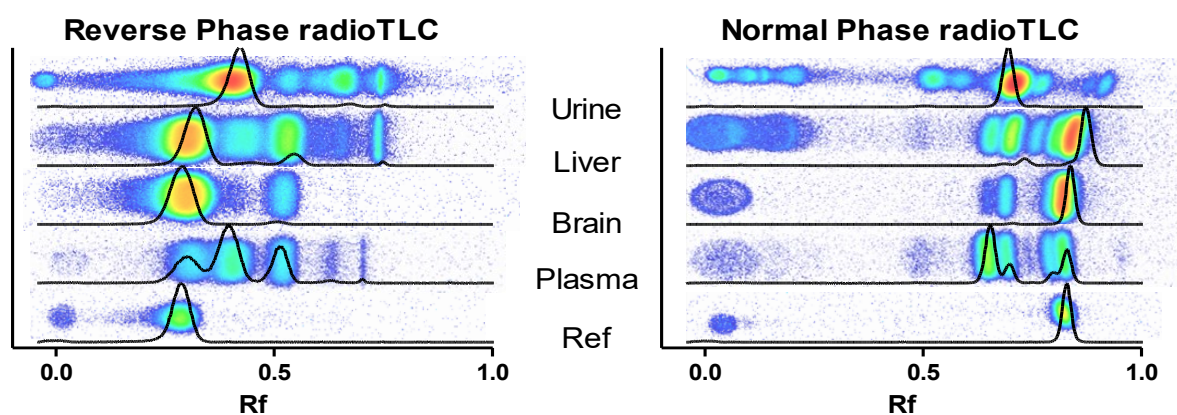


Figure 28: radioTLC chromatograms overlaid with autoradiography of TLC plates taken from Rat 2

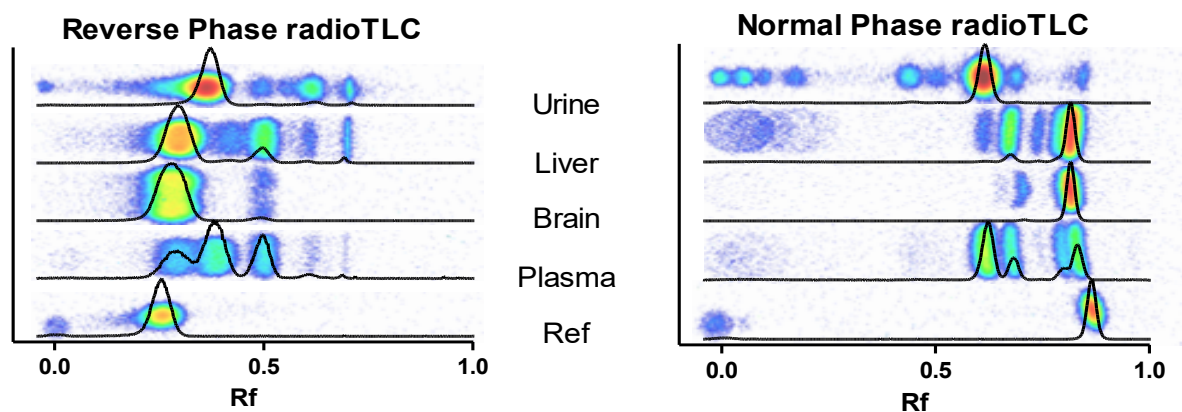


Figure 29: radioTLC chromatograms overlaid with autoradiography of TLC plates taken from Rat 3

The radiometabolism of [ $^{18}\text{F}$ ]UCB-J was also analysed using radioHPLC, where the degree of radiometabolism can be detected by comparing the sample chromatograms to the reference chromatogram presented in figure 30. The reference chromatogram was created by injecting a 1:4 [ $^{18}\text{F}$ ]UCB-J:acetonitrile sample containing  $0.375 \text{ MBq } \mu\text{L}^{-1}$  of activity to the HPLC. In figure 31 we see a major peak in the radioactivity chromatogram at around 8.5 minutes corresponding to the injected [ $^{18}\text{F}$ ]UCB-J. Alignment with this peak is the indicator for the presence of non-metabolized [ $^{18}\text{F}$ ]UCB-J in the sample.

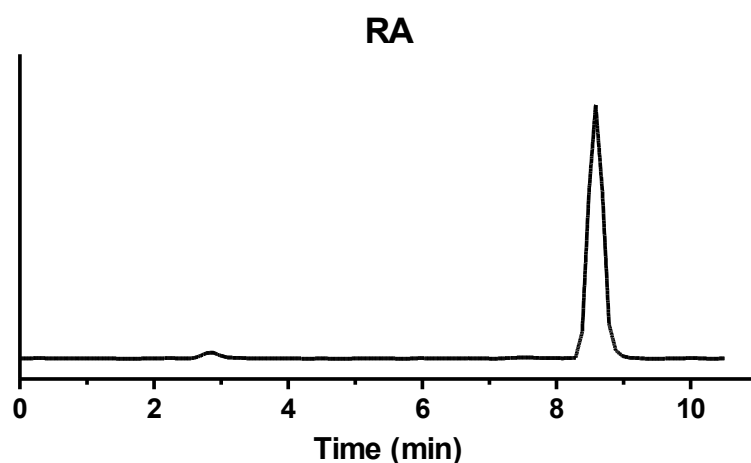


Figure 30: [ $^{18}\text{F}$ ]UCB-J reference radioHPLC chromatogram

The radioHPLC chromatograms from rat 1's plasma, brain, urine and liver samples are presented in figure 31. There we can see from the plasma chromatogram that multiple peaks corresponding to several radiometabolites are present. In addition to this un-metabolized [ $^{18}\text{F}$ ]UCB-J is also present as can be seen from the peak at 8.5 minutes that aligns with the reference. We can also see from the brain chromatogram that the major peak corresponds to the reference chromatogram indicating that present [ $^{18}\text{F}$ ]UCB-J is mostly un-metabolized. In the urine chromatogram we can see that the sample contains mostly metabolized [ $^{18}\text{F}$ ]UCB-J as the major peak does not correspond to the reference. The liver chromatogram shows a large peak aligning with the reference indicating the presence of non-metabolized [ $^{18}\text{F}$ ]UCB-J, but also several smaller peaks that indicate multiple radiometabolites to be present.

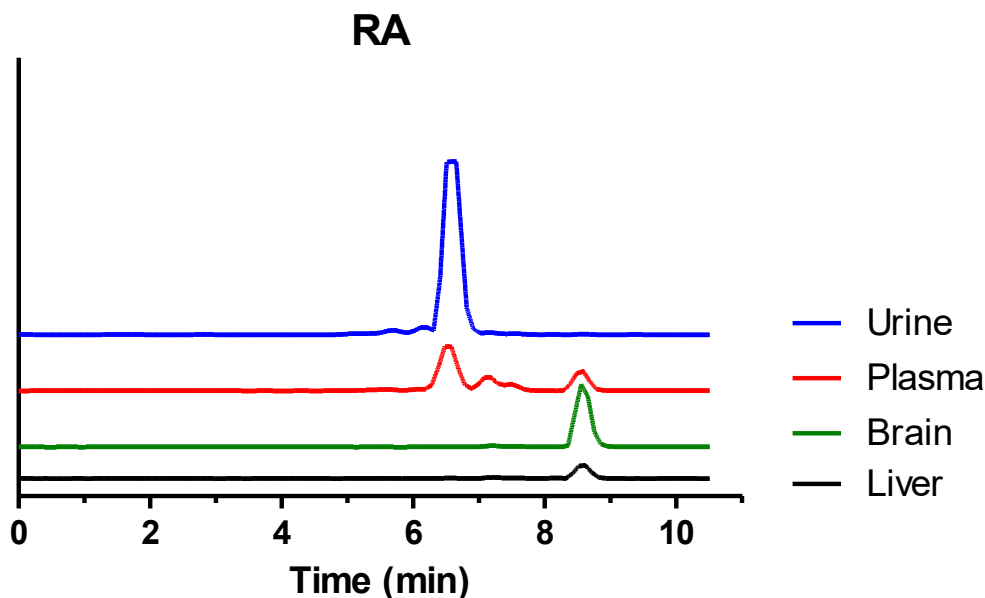


Figure 31: RadioHPLC chromatograms of Brain, Plasma and Urine samples from rat 1

The radioHPLC chromatogram from the plasma, brain and urine samples of rat 2 are presented in figure 32. We can see that the results from the plasma chromatogram are similar to the sample from rat 1 showing both multiple radiometabolites and non-metabolized [ $^{18}\text{F}$ ]UCB-J to be present. The brain sample of rat 2 that matches also closely with the brain sample from rat 1, indicating mostly non-metabolized [ $^{18}\text{F}$ ]UCB-J. The urine sample of rat 2 again matches closely with the radioHPLC chromatogram from rat 1's urine sample, indicating mostly metabolized [ $^{18}\text{F}$ ]UCB-J to be present.

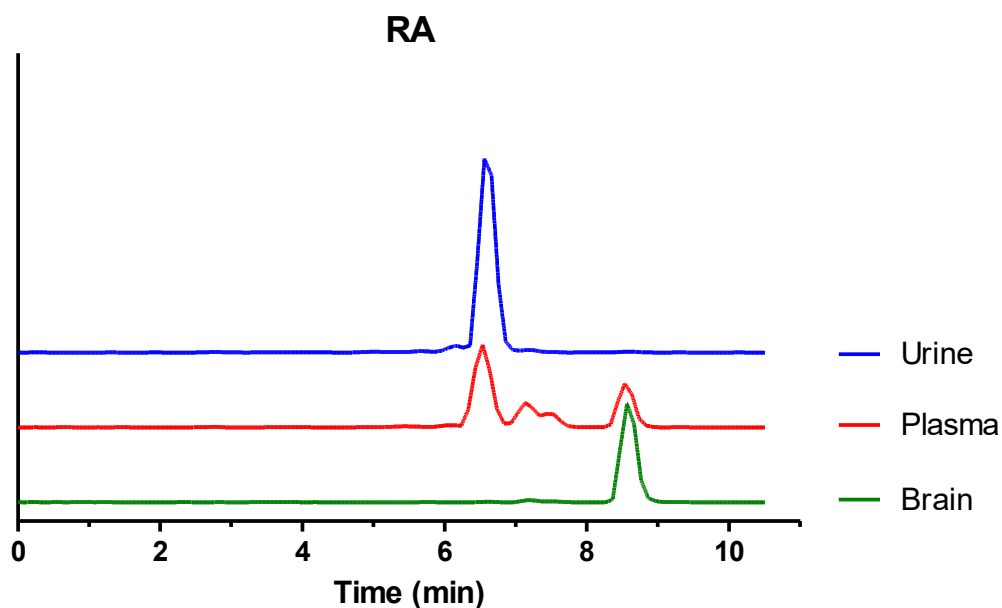


Figure 32: Plasma sample radioHPLC chromatogram from rat 2

Figure 33 shows the radioHPLC chromatogram from the plasma, brain and urine samples of rat 3. The plasma chromatogram matches the chromatograms of the previous two samples from rat 1 and 2, indicating presence of both several radiometabolites and non-metabolized [ $^{18}\text{F}$ ]UCB-J. The brain chromatogram again shows a close match the samples from rat 1 and 2, showing a peak that aligns with the reference and indicating the presence of mostly non-metabolized [ $^{18}\text{F}$ ]UCB-J. The urine chromatogram matches the results from rat 1 and rat 2 indicating mostly metabolized [ $^{18}\text{F}$ ]UCB-J to be present.

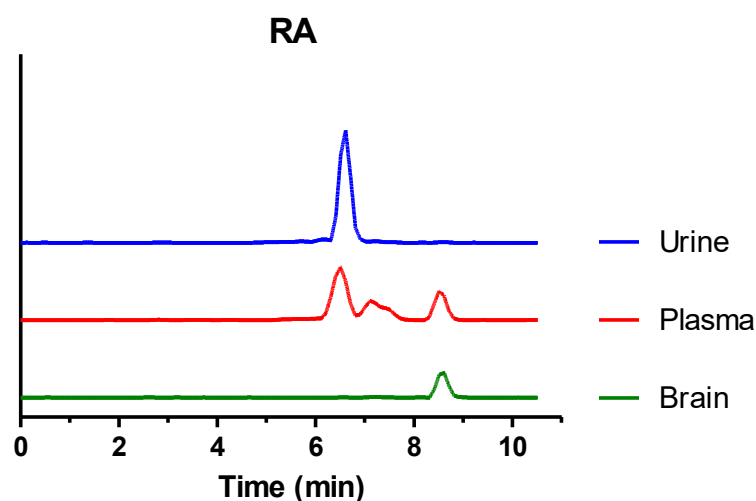


Figure 33: Plasma sample radioHPLC chromatogram from rat 3

From these radioHPLC chromatograms we can see that they largely align with each other, suggesting that the brain sample contains mostly un-metabolized [ $^{18}\text{F}$ ]UCB-J and the urine mostly metabolized [ $^{18}\text{F}$ ]UCB-J while the plasma and liver contain both. This corresponds to the results obtained from the radioTLC tests. In future tests radioHPLC might provide more replicable results as it is a more robust method than radioTLC.

## 4 Conclusions

The synthesis of the hypervalent iodine compounds **1**, **2** and **4** can be deemed successful based on the results of the  $^1\text{H}$ -NMR spectra, the synthesis of compound **3** was not successful. The synthesis of [ $^{18}\text{F}$ ]UCB-J was tested for each of the compounds **1**, **2**, and **4** in the reactions 1-8, the results of which were analysed using radioHPLC. Based on the results of the radioHPLC analysis, no reaction was successful in synthesizing [ $^{18}\text{F}$ ]UCB-J. A possible reason for the unsuccessful synthesis could be the instability of the I-F bond to water when present with TBAF, a phenomenon that is also used to detect minuscule amounts of water in samples<sup>52</sup>.

The results of the bio-distribution of activity show that most activity is concentrated in the urine, liver, cortex and brain of the test animals one hour after injection. The radioTLC study of radiometabolites shows the greatest degree of radiometabolism in the urine and plasma samples, with the least amount of radiometabolism in the brain and liver samples of the test animals. In addition, the reverse phase radioTLC afforded better separation of peaks than the normal phase radioTLC method. This indicates that the metabolites are mostly polar compounds and interact more with the polar material of the reverse phase TLC plates than the non-polar normal phase TLC plates. The radioHPLC results of the radiometabolite study show that the urine samples contain the mostly metabolized [ $^{18}\text{F}$ ]UCB-J, with the plasma samples showing the second most radiometabolism of [ $^{18}\text{F}$ ]UCB-J. The brain samples of the radioHPLC radiometabolism study show mostly un-metabolized [ $^{18}\text{F}$ ]UCB-J with the singular liver sample containing also a large degree of un-metabolized [ $^{18}\text{F}$ ]UCB-J. The results of the radioHPLC radiometabolism study might prove more replicable than the results of the radioTLC study due to the more robust HPLC method.

The results of the radiometabolism study are largely in alignment with each other, indicating that [ $^{18}\text{F}$ ]UCB-J does not present a large degree of radiometabolism in the brain of the test animals, leading to good resolution when potentially conducting PET-imaging of the synaptic vesicle glycoprotein 2A in the brain. In addition, the result show that the urine of the test animals contains mostly radiometabolized [ $^{18}\text{F}$ ]UCB-J, indicating it to be the major secretion pathway for radiometabolized [ $^{18}\text{F}$ ]UCB-J.

Though the synthesis of [ $^{18}\text{F}$ ]UCB-J using [ $^{18}\text{F}$ ]fluoro-benziodoxole produced from the various hypervalent iodine compounds **1**, **2** and **4** did not work, the promise of a simple umpolung performing electrophilic  $^{18}\text{F}$ -fluorinating reagent is still an attractive one and these results are not by themselves enough to discount [ $^{18}\text{F}$ ]fluoro-benziodoxole. Further testing of [ $^{18}\text{F}$ ]fluoro-benziodoxole would still

need to be performed to find out the full scope of what [ $^{18}\text{F}$ ]fluoro-benziodoxole is capable of in the field of radiopharmaceutical fluorine-18 chemistry.

## 5 References

1. Vera Ruiz H. Report of an International Atomic Energy Agency's consultants' meeting on fluorine 18: Reactor production and utilization. *Int J Radiat Appl Instrumentation Part.* 1988;39(1):31-39. doi:10.1016/0883-2889(88)90089-5
2. Bergman J, Solin O. Fluorine-18-labeled fluorine gas for synthesis of tracer molecules. *Nucl Med Biol.* 1997;24(7):677-683. doi:10.1016/S0969-8051(97)00078-4
3. Krzyczmonik A, Keller T, Kirjavainen AK, Forsback S, Solin O. Vacuum ultraviolet photon-mediated production of [18F]F<sub>2</sub>. *J Label Compd Radiopharm.* 2017;60(4):186-193. doi:10.1002/jlcr.3489
4. Diksic M, Farrokhzad S. New synthesis of fluorine-18-labeled 6-fluoro-L-dopa by cleaving the carbon-silicon bond with fluorine. *J Nucl Med.* 1985;26(11):1314-1318.
5. Nickles RJ, Daube ME, Ruth TJ. An 18O<sub>2</sub> target for the production of [18F]F<sub>2</sub>. *Int J Appl Radiat Isot.* 1984;35(2):117-122. doi:10.1016/0020-708X(84)90194-7
6. Neirinckx RD, Lambrecht RM, Wolf AP. Cyclotron isotopes and radiopharmaceuticals- XXV An anhydrous 18F-fluorinating intermediate: Trifluoromethyl hypofluorite. *Int J Appl Radiat Isot.* 1978;29(4-5):323-327. doi:10.1016/0020-708X(78)90062-5
7. Cady GH, Khayat SI, Willson KS. Trifluoromethyl Hypofluorite. *Inorg Synth.* 2007;8(2):165-170. doi:10.1002/9780470132395.ch43
8. Ehrenkaufner RE, MacGregor RR. Synthesis of [18F]perchloryl fluoride and its reactions with functionalized aryl lithiums. *Int J Appl Radiat Isot.* 1983;34(3):613-615. doi:10.1016/0020-708X(83)90064-9
9. Jared L. The preparatory manual of explosives. Published online 2007:58-59.
10. Hiller A, Fischer C, Jordanova A, Patt JT, Steinbach J. Investigations to the synthesis of n.c.a. [18F]FCIO<sub>3</sub> as electrophilic fluorinating agent. *Appl Radiat Isot.* 2008;66(2):152-157. doi:10.1016/j.apradiso.2007.08.016
11. Chirakal R, Firmau G, Couse J, Garnett ES. Radiofluorination with 18F-labelled acetyl hypofluorite: [18F]L-6-fluorodopa. *Int J Appl Radiat Isot.* 1984;35(7):651-653. doi:10.1016/0020-708X(84)90111-X
12. Ori Lerman, Yitzhak Tor SR. Fluorination of Activated Aromatic Rings. *J Org Chem.* 1981;46(5):4629-4631.
13. Adam M, Ruth T, Jivan S, Pate B. Fluorination of aromatic compounds with F<sub>2</sub> and acetyl hypofluorite: synthesis of 18F-aryl fluorides by cleavage of aryl-tin bonds [1]. *J Fluor Chem.* 1984;25(3):329-337. doi:10.1016/S0022-1139(00)81207-5
14. Adam MJ, Grierson JR, Ruth TJ, Jivan S. Reaction of [18F]acetyl hypofluorite with derivatives of dihydroxyphenylalanine: Synthesis of l-[18F]6-fluorodopa. *Int J Radiat Appl Instrumentation Part.* 1986;37(8):877-882. doi:10.1016/0883-2889(86)90286-8

15. Namavari M, Bishop A, Satyamurthy N, Bida G, Barrio JR. Regioselective radiofluorodestannylation with  $[^{18}\text{F}]\text{F}_2$  and  $[^{18}\text{F}]\text{CH}_3\text{COOF}$ : A high yield synthesis of 6- $[^{18}\text{F}]$ fluoro-L-dopa. *Int J Radiat Appl Instrumentation Part.* 1992;43(8):989-996. doi:10.1016/0883-2889(92)90217-3
16. Szajek LP, Channing MA, Eckelman WC. Automated synthesis of 6- $[^{18}\text{F}]$ fluoro-L-DOPA using modified polystyrene supports with bound 6-mercuric DOPA precursors. *Appl Radiat Isot.* 1998;49(7):795-804. doi:10.1016/S0969-8043(97)00304-7
17. Adam MJ, Ruth TJ, Grierson JR, Abeysekera B, Pate BD. Routine synthesis of L- $[^{18}\text{F}]$ 6-fluorodopa with fluorine-18 acetyl hypofluorite. *J Nucl Med.* 1986;27(9):1462-1466. PMID: 3091786
18. Chaly T, Diksic M. High yield synthesis of 6- $[^{18}\text{F}]$ fluoro-L-dopa by regioselective fluorination of protected L-dopa with  $[^{18}\text{F}]$ acetyl hypofluorite. *J Nucl Med.* 1986;27(12):1896-1901. PMID: 3097278
19. Shiue CY, Salvadori PA, Wolf AP, Fowler JS, MacGregor RR. A new improved synthesis of 2-deoxy-2- $[^{18}\text{F}]$ fluoro-D-glucose from 18F-labeled acetyl hypofluorite. *J Nucl Med.* 1982;23(10):899-903. PMID: 7119884
20. Ehrenkauf RE, Potocki JF, Jewett DM. Simple synthesis of F-18-labeled 2-fluoro-2-deoxy-d-glucose: Concise communication. *J Nucl Med.* 1984;25(3):333-337. PMID: 6699724
21. Wang HE, Liao AH, Deng WP, et al. Evaluation of 4-borono-2-18F-fluoro-L-phenylalanine-fructose as a probe for boron neutron capture therapy in a glioma-bearing rat model. *J Nucl Med.* 2004;45(2):302-308. PMID: 14960653
22. Bergman J, Johnström P, Haaparanta M, et al. Radiolabelling of 2-oxoquazepam with electrophilic 18F prepared from  $[^{18}\text{F}]$ fluoride. *Appl Radiat Isot.* 1995;46(10):1027-1034. doi:10.1016/0969-8043(94)00127-L
23. Mathis CA, Shulgin AT, Yano Y, Sargent T. 18F-labelled N,N-dimethylamphetamine analogues for brain imaging studies. 1986;37(8):865-872. doi:10.1016/0883-2889(86)90284-4
24. Visser GWM, Bijma AT, Dijkman JAR, et al. The in vitro and in vivo behaviour of 18F-labelled 5-fluoro-5,6-dihydrouracil nucleosides. 1989;16(4):351-357. doi:10.1016/0883-2897(89)90098-6
25. Tada M, Matsuzawa T, Yamaguchi K, et al. Synthesis of 18F-labelled 2-deoxy-2-fluoro-d-galactopyranose using the acetyl hypofluorite procedure, *Carbohydr Res.* 1987;161(2):314-317, doi:10.1016/S0008-6215(00)90089-2.
26. Mohammad N, Satyamurthy N, Phelps E, Barrio JR. Synthesis of 6- $[^{18}\text{F}]$  and 4- $[^{18}\text{F}]$  Fluoro-L-m-tyrosines via Regioselective Radiofluorodestannylation. *Appl Radiat Isot.* 1993;44(3):527-536. doi:10.1016/0969-8043(93)90165-7.
27. Tius MA. Xenon difluoride in synthesis. *Tetrahedron.* 1995;51(24):6605-6634. doi:10.1016/0040-4020(95)00362-C
28. Schrobilgen G, Firnau G, Chirakal R, Garnett ES. Synthesis of  $[^{18}\text{F}]\text{XeF}_2$ , a novel agent for the preparation of 18F-radiopharmaceuticals. *J Chem Soc Chem Commun.* 1981;(4):198-199. doi:10.1039/C39810000198

29. Sood S, Firna G, Garnett ES. Radiofluorination with xenon difluoride: A new high yield synthesis of [18F]2-fluoro-2-deoxy-d-glucose. *Int J Appl Radiat Isot.* 1983;34(4):743-745. doi:10.1016/0020-708X(83)90254-5
30. Oberdorfer F, Hofmann E, Maier-Borst W, Preparation of a new 18F-labelled precursor: 1-[18F]fluoro-2-pyridone. *Int J Rad Appl Instr A.* 1988;39(7):685-688. doi:10.1016/0883-2889(88)90058-5
31. Satyamurthy N, Bida GT, Phelps ME, Barrio JR. N-[18F]fluoro-N-alkylsulfonamides: Novel reagents for mild and regioselective radiofluorination. *Int J Radiat Appl Instrumentation Part.* 1990;41(8):733-738. doi:10.1016/0883-2889(90)90020-H
32. Teare H, Robins EG, Årstad E, Luthra SK, Gouverneur V. Synthesis and reactivity of [18F]-N-fluorobenzenesulfonimide. *Chem Commun.* 2007;(23):2330-2332. doi:10.1039/b701177f
33. Nodwell MB, Yang H, Čolović M, et al. 18F-Fluorination of Unactivated C-H Bonds in Branched Aliphatic Amino Acids: Direct Synthesis of Oncological Positron Emission Tomography Imaging Agents. *J Am Chem Soc.* 2017;139(10):3595-3598. doi:10.1021/jacs.6b11533
34. Yuan Z, Nodwell MB, Yang H, et al. Site-Selective, Late-Stage C-H 18F-Fluorination on Unprotected Peptides for Positron Emission Tomography Imaging. *Angew Chemie - Int Ed.* 2018;57(39):12733-12736. doi:10.1002/anie.201806966
35. Oberdorfer F, Hofmann E, Maier-Borst W. Preparation of 18F-labelled N-fluoropyridinium triflate. *J Label Compd Radiopharm.* 1988;25(9): 999. doi:10.1002/jlcr.2580250912
36. Banks RE, Besheesh MK, Mohialdin-Khaffaf SN, Sharif I. N-Halogeno compounds. Part 18. 1-Alkyl-4-fluoro-1,4-diazoniabicyclo[2.2.2]octane salts: user-friendly site-selective electrophilic fluorinating agents of the N-fluoroammonium class. *J Chem Soc, Perkin Trans 1.* 1996; (16): 2069-2076. doi:10.1039/P19960002069
37. Hart JJ, Syvret RG. Industrial scale production of Selectfluor™ fluorination agent: From initial concept to full scale commercial production in a 5 year period. *J Fluor Chem.* 1999;100(1-2):157-161. doi:10.1016/S0022-1139(99)00199-2
38. Teare H, Robins EG, Kirjavainen A, et al. Radiosynthesis and evaluation of [18F]Selectfluor bis(triflate). *Angew Chemie - Int Ed.* 2010;49(38):6821-6824. doi:10.1002/anie.201002310
39. Stenhagen ISR, Kirjavainen AK, Forsback SJ, et al. [18F]Fluorination of an arylboronic ester using [18F]selectfluor bis(triflate): Application to 6-[18F]fluoro-l-DOPA. *Chem Commun.* 2013;49(14):1386-1388. doi:10.1039/c2cc38646a
40. Kirjavainen AK, Forsback S, López-Picón FR, et al. 18F-labeled norepinephrine transporter tracer [18F]NS12137: radiosynthesis and preclinical evaluation. *Nucl Med Biol.* 2018;56:39-46. doi:10.1016/j.nucmedbio.2017.10.005
41. Keller T, Krzyczmonik A, Forsback S, et al. Radiosynthesis and Preclinical Evaluation of [18F]F-DPA, A Novel Pyrazolo[1,5a]pyrimidine Acetamide TSPO Radioligand, in Healthy Sprague Dawley Rats. *Mol Imaging Biol.* 2017;19(5):736-745. doi:10.1007/s11307-016-1040-z

42. Krzyczmonik A, Keller T, López-Picón FR, et al. Radiosynthesis and Preclinical Evaluation of an  $\alpha$ 2A-Adrenoceptor Tracer Candidate, 6-[18F]Fluoro-marsanidine. *Mol Imaging Biol.* 2019;21(5):879-887. doi:10.1007/s11307-019-01317-6
43. Lee E, Kamlet AS, Powers DC, et al. A fluoride-derived electrophilic late-stage fluorination reagent for PET imaging. *Science* (80- ). 2011;334(6056):639-642. doi:10.1126/science.1212625
44. Kamlet AS, Neumann CN, Lee E, et al. Application of Palladium-Mediated 18F-Fluorination to PET Radiotracer Development: Overcoming Hurdles to Translation. *PLoS One.* 2013;8(3):1-10. doi:10.1371/journal.pone.0059187
45. Cortés González MA, Nordeman P, Bermejo Gómez A, et al. Fluoro-benziodoxole: A no-carrier-added electrophilic fluorinating reagent. Rapid, simple radiosynthesis, purification and application for fluorine-18 labelling. *Chem Commun.* 2018;54(34):4286-4289. doi:10.1039/c8cc00526e
46. Cortés González MA, Jiang X, Nordeman P, Antoni G, Szabó KJ. Rhodium-mediated 18F-oxyfluorination of diazoketones using a fluorine-18-containing hypervalent iodine reagent. *Chem Commun.* 2019;55(89):13358-13361. doi:10.1039/c9cc06905d
47. Nabulsi NB, Mercier J, Holden D, et al. Synthesis and preclinical evaluation of 11C-UCB-J as a PET tracer for imaging the synaptic vesicle glycoprotein 2A in the brain. *J Nucl Med.* 2016;57(5):777-784. doi:10.2967/jnumed.115.168179
48. Li S, Cai Z, Zhang W, et al. Synthesis and in vivo evaluation of [18F]UCB-J for PET imaging of synaptic vesicle glycoprotein 2A (SV2A). *Eur J Nucl Med Mol Imaging.* 2019;46(9):1952-1965. doi:10.1007/s00259-019-04357-w
49. Keller T, Kerminen E, Forsback S, Kirjavainen A, Solin O. Synthesis of [18F]UCB-J. *Nucl Med Biol.* 2022;108-109(334210):S82. doi:10.1016/s0969-8051(22)00196-2
50. Rabah GA, Koser GF. Facile synthetic entry into the 1,3-dihydro-3-methyl-3-phenyl-1,2-benziodoxole family of  $\lambda$ 3-iodanes. *Tetrahedron Lett.* 1996;37(36):6453-6456. doi:10.1016/0040-4039(96)01436-0
51. Geary GC, Hope EG, Singh K, Stuart AM. Electrophilic fluorination using a hypervalent iodine reagent derived from fluoride. *Chem Commun.* 2013;49(81):9263-9265. doi:10.1039/c3cc44792h
52. Sun H, Wang B, Dimagno SG. A method for detecting water in organic solvents. *Org Lett.* 2008;10(20):4413-4416. doi:10.1021/ol8015429

## 6 Attachments

### 6.1 List of attachments:

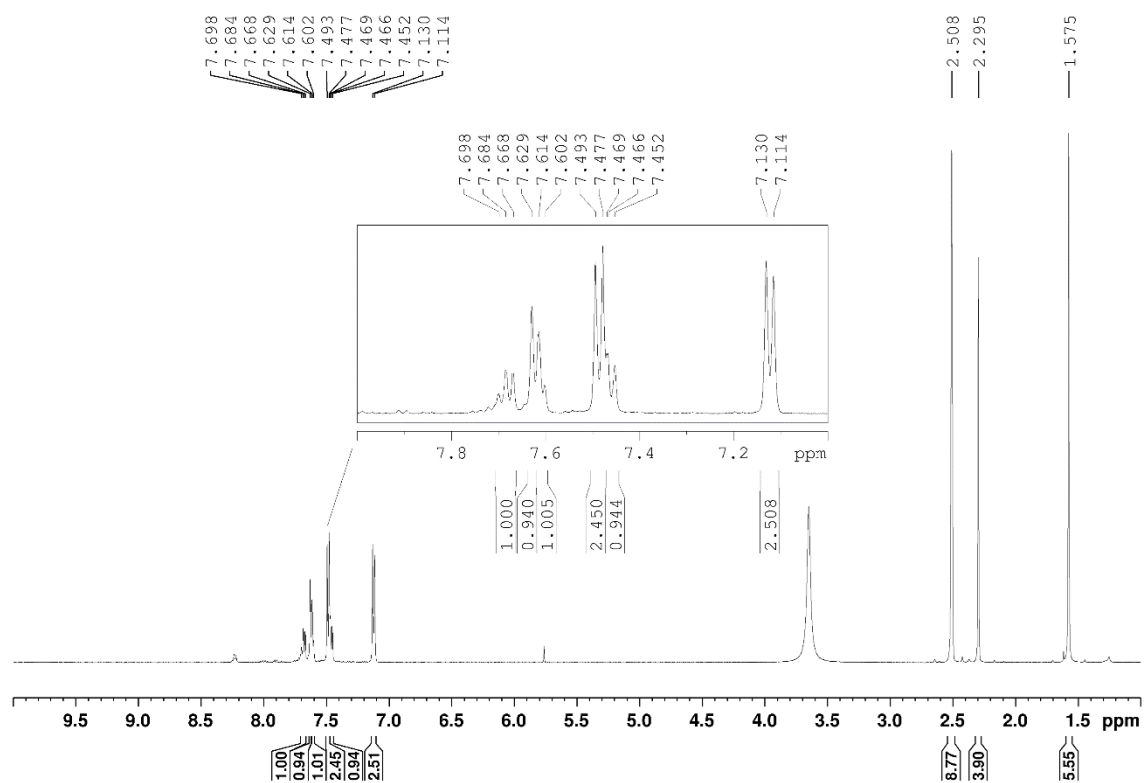
Attachment 1:  $^1\text{H}$ -NMR spectrum of 1-tosyloxy-3,3-dimethyl-1,3-dihydro- $\lambda^3$ -benzo[d][1,2]iodoxole (1)

Attachment 2:  $^1\text{H}$ -NMR spectrum of 3,3-dimethyl- $1\lambda^3$ -benzo[d][1,2]iodaoxol-1(3H)-yl 2,2,2-trifluoroacetate (2)

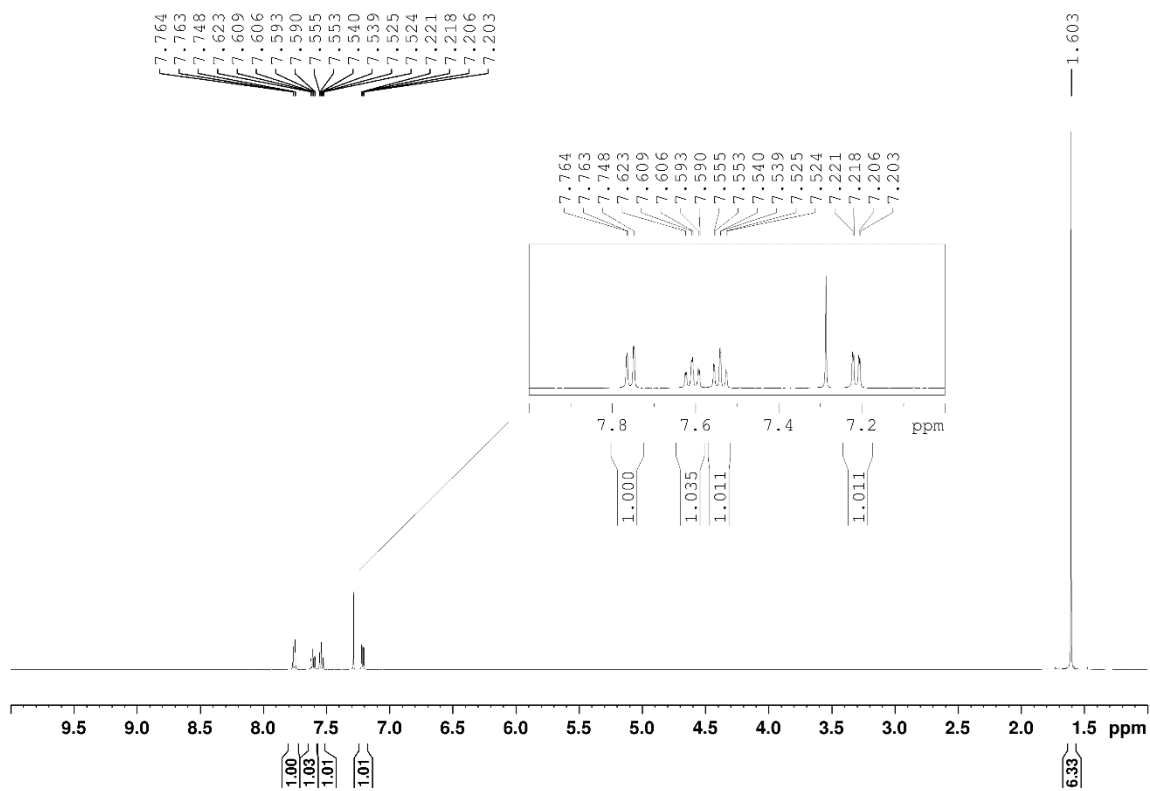
Attachment 3:  $^1\text{H}$ -NMR spectrum of 3,3-dimethyl- $1\lambda^3$ -benzo[d][1,2]iodaoxol-1(3H)-yl acetate (3)

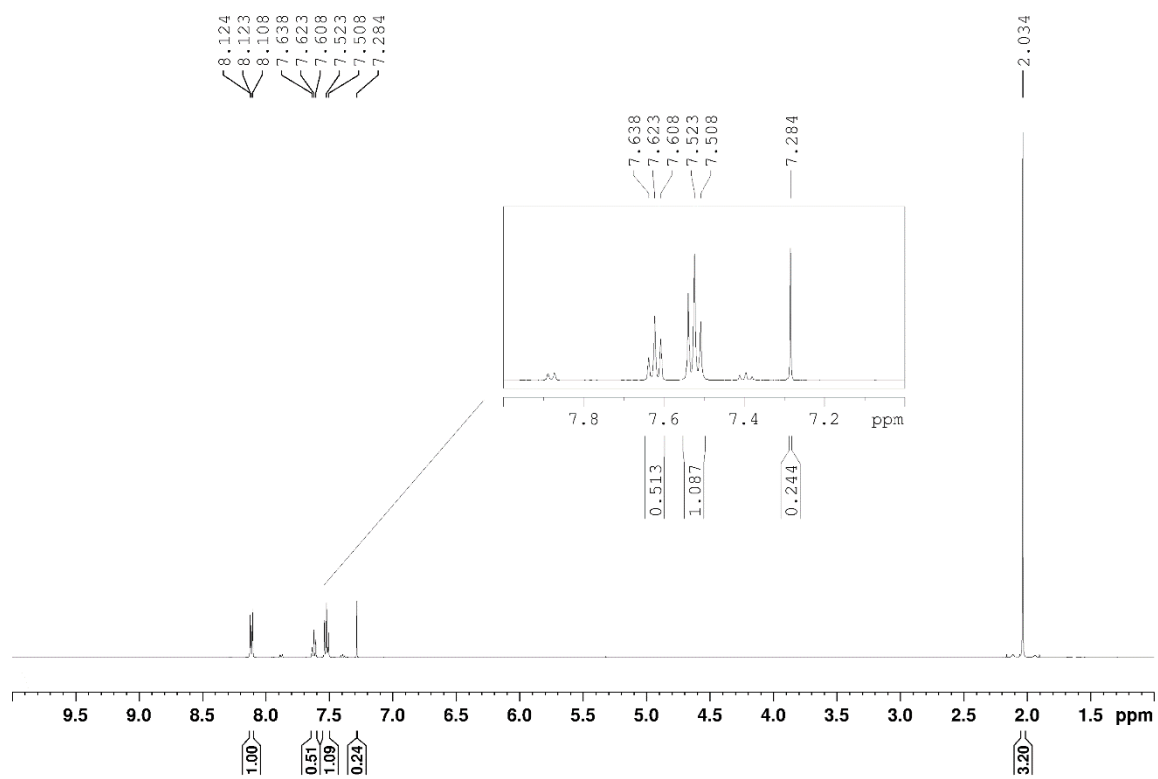
Attachment 4:  $^1\text{H}$ -NMR spectrum of 1-(chloromethyl)-4-(((3,3-dimethyl- $1\lambda^3$ -benzo[d][1,2]iodooxol-1(3H)-yl)oxy)carbonyl)-1,4-diazabicyclo[2.2.2]octane-1,4-dium (4)

Attachment 1:  $^1\text{H-NMR}$  spectrum of 1-tosyloxy-3,3-dimethyl-1,3-dihydro- $\lambda^3$ -benzo[d][1,2]iodoxole (**1**)



Attachment 2:  $^1\text{H-NMR}$  spectrum of 3,3-dimethyl-1 $\lambda^3$ -benzo[d][1,2]iodaoxol-1(3H)-yl 2,2,2-trifluoroacetate (**2**)



Attachment 3:  $^1\text{H-NMR}$  spectrum of crude product of precursor **3** synthesis

Attachment 4:  $^1\text{H-NMR}$  spectrum of 1-(chloromethyl)-4-(((3,3-dimethyl-1 $\lambda^3$ -benzo[d][1,2]iodooxol-1(3H)-yl)oxy)carbonyl)-1,4-diazabicyclo[2.2.2]octane-1,4-dium (4)

